THE EARLY PROTEROZOIC SAARI-KIEKKI GREENSTONE BELT: A REPRESENTATIVE OF THE SARIOLA GROUP AT KUHMO, EASTERN FINLAND

ERKKI J. LUUKKONEN

LUUKKONEN, ERKKI J., 1989: The early Proterozoic Saari-Kiekki greenstone belt: A representative of the Sariola Group at Kuhmo, Eastern Finland. *Bull. Geol. Soc. Finland 61, Part 2,* 161—187.

The early Proterozoic Saari-Kiekki greenstone belt in Kuhmo, eastern Finland, is the deformed remnant of a NW—SE-trending elongate structural basin c. 15 km long and up to 3 km wide. It is correlated with the Sariola Group in eastern and northeastern Finland as well as with the Sumi-Sariola Group in Soviet Karelia, and is thus one representative of this oldest unit of the Karelia Supergroup preserved in Central Finland.

The volcano-sedimentary sequence of the belt was deposited in terrestial to fluvial environments on late Archaean granitoids and migmatites, in a fault-bounded basin. The basin-margin faults belong to a regional system of dextral strike-slip faults, which were active both prior to (= late Archaean time), during and after the basin formation (= early Proterozoic time). Locally the marginal zones of the basin are characterized by tectonic—eluvial granitoid breccia hundreds of metres thick, which contain some arkosic layers (= Latvalampi Formation). Subaereal or partly subaqueous basalts, basaltic andesites and andesites were deposited longitudinally in the centre of the basin (= Kaita-Kiekki Formation). In many places the volcanic suite is overlain by the sublitharenites, arkosic sandstones—conglomerates and polymictic conglomerates (= Pötsölampi Formation). The whole belt is cut by NW—SE — or NNW—SSE-trending early Proterozoic metadiabase dykes.

U-Pb zircon and titanite isotopic data for the metadiabase dyke indicate that the Saari-Kiekki greenstone belt was deposited before 2209 ± 11 Ma. The problematic calc-alkaline trend of the Kaita-Kiekki intermediate volcanites associated with the intracratonic strike-slip fault system is interpreted to be a consequence of late Archaean crustal contamination of basaltic magma at depth during its uprise.

Regional dextral E—SE-trending strike-slip faulting, overthrusting from west to east, open to tight folding, a strong west plunging lineation and the development of the Saari-Kiekki greenstone belt, record an important stage of early Proterozoic reactivation in the late Archaean basement. The early Proterozoic structural patterns can be divided into three deformational phases and the metamorphism during that time seldom exceeded the lower amphibolite facies.

Key words: greenstone belts, stratigraphy, metavolcanic rocks, metasedimentary rocks, chemical composition, deformation, absolute age, Proterozoic, Sariolian, Saari-Kiekki, Kuhmo, Finland.

Erkki J. Luukkonen: Geological Survey of Finland, P.O. Box 1237, SF-70701 Kuopio, Finland.

Introduction

The formations composed of diamictites and unsorted and chemically unweathered conglomerates underlying the early Proterozoic Jatuli formations were first referred to as Sariola by Eskola as early as 1919. In 1941 he revised his Sariola concept by including arkosites and arkosic schists in the upper part of the Sariola stratigraphy, and with his ideas concerning chemical weathering during the Sariolan. Väyrynen (1933, 1954) assumed that the Sariola conglomerates were deposited from chemically unweathered, mechanically eroded material, in a terrain of high relief. As soon as terrain became more level, chemical weathering was prevalent so that in many places, the Sariola conglomerates are seen to be weathered in situ without redeposition. This opinion was also accepted by Eskola in 1963. Ojakangas (1965) interpreted Sariola conglomerates to be fluvial and deposited in an environment where mechanical erosion surpassed the chemical weathering. Pekkarinen (1979) pointed out that the Prejatulian (= Sariolan) breccia-conglomerates were almost coeval with the early Karelian weathering crust and that the oldest arkosic suite was fluvial and deposited under desert-like conditions. During this decade, glaciogenic features have been found in the Sariola Formations of eastern Finland (Marmo and Ojakangas 1983,1984; Marmo 1986) and, in contrast to Eskola's original Sariola definition, volcanic units are also included (Laajoki 1973,1980; Meriläinen 1980; Luukkonen and Lukkarinen 1986; Strand 1988).

In Soviet Karelia many Sariola-type formations have been reported, and the Sariola problem has long debated by Karelian geologists. Previously, according to the prevalent Soviet interpretation the Sumi Group is the oldest part of the sequence, and composed of basaltic, andesitic-basaltic, andesitic-dacitic, and rhyolitic metavolcanics together with quartzites, conglomerates and schists. The sequence is intruded by c. 2450 Ma old layered gabbro-anorthosites, pyroxene granites and quartz-porphyry dykes. In many places the Sumi Group is overlain by conglomerates, arkosic quartzites and tuffitic sandstones of the Sariola Group , correlative with the Finnish Sariola formations (Sokolov and Stenar 1980; Kratz and Mitrofanov 1980). In recent years on the basis of lithostratigraphic correlations the Sumi-Sariola in Soviet Karelia has been classified into several stratotypes (Kulikov and Golubev 1984).

a) Seletsky-stratotype considered to resemble the Sariola described by Eskola (1941).

b) Kumsa-stratotype typically consisting of thick basaltic and andesitic-basaltic lava flows alternating in the upper part with mixed volcanogenic sedimentary rocks.

c) Paanajärvi-stratotype having much in common with the Seletsky and the Kumsa-stratotypes, but containing in addition felsic potassium-rich volcanic rocks.

This paper presents the results of recent mapping and structural, lithogeochemical and isotopic studies of the well preserved though metamorphosed Sariolan volcanic and sedimentary succession in the Saari-Kiekki greenstone belt, which was previously poorly known because of its remote location near the Soviet border in eastern Kuhmo. The area had however, been mapped earlier by Wilkman (1900—1909), and the Saari-Kiekki metabasites and metaconglomerates are mentioned in the explanation to the geological map of Nurmes map sheet area (Wilkman 1921), but not in the sense of belonging to the Sariola Group.

General geology

The stratigraphic and structural interpretation of the Saari-Kiekki greenstone belt is hindered by the virtual absence of good outcrops in the NW central part of the studied area, and the mylonitic contacts between the formations. The lithological, lithostratigraphical and structural figures (Figs 1, 6, 25) presented here should therefore be considered in this light.
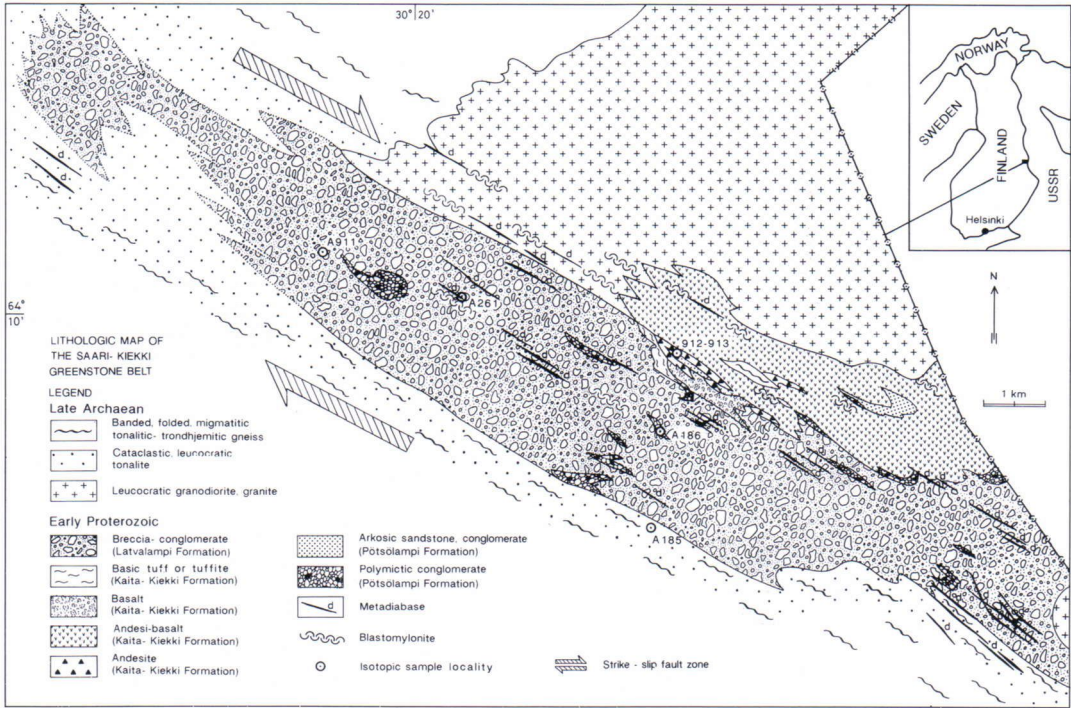
Fig. 1. Simplified map showing the distribution of lithologies in the Saari-Kiekki greenstone belt.

In the area studied the supracrustal rocks are preserved in a southeast-trending synclinorium having faulted margins (Fig. 1). It borders against the Soviet Union, but the extent to which it continues into Soviet Karelia is unknown. In Finland the belt is c. 15 km long and some 3 km wide.

The late Archaean basement complex to the south of the greenstone belt consists of late Archaean polydeformed, migmatitic tonalites-trondhjemites (Fig. 2), which towards the mar-
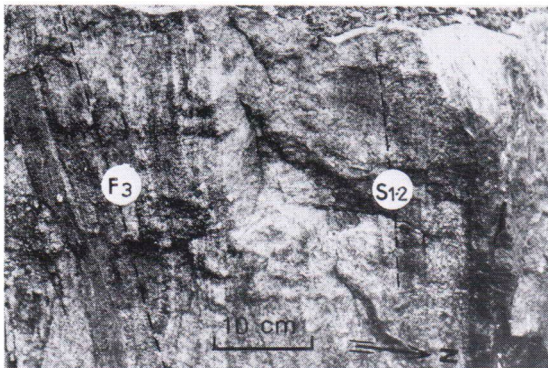

Fig. 2. Banded, folded tonalite-trondhjemite, showing composite foliation S_{1-2}, banding caused by late Archaean metamorphic (M_{1-2}) segregation, and almost isoclinal F_3 folding.
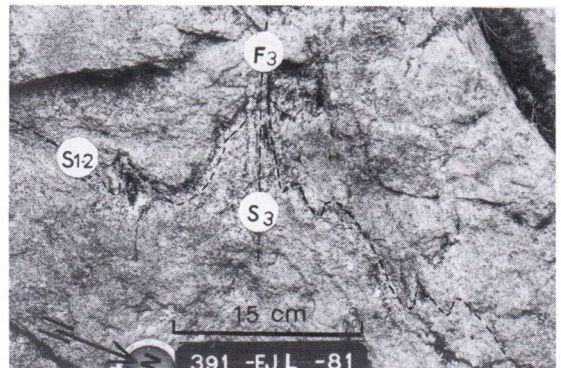

Fig. 3. Cataclastic, leucocratic tonalite with xenolith of totally recrystallized late Archaean banded tonalite-trondhjemite showing late Archaean F_3 chevron type folding with S_3 axial planar foliation.

gin of the belt, grade into foliated, cataclastic leu-
cocratic tonalite containing migmatitic tonalite-
trondhjemite enclaves (Fig. 3).

Zircon grains from the leucocratic tonalite are
rather long (elongation ratios of 5:1 or more),
clear and vary from anhedral to subhedral in
shape. The U-Pb data for four zircon fractions
(Table 2, sample A185) from this rock type de-
fine a chord which gives an upper intercept with
the concordia at 2784 ± 4 Ma, and a lower in-
tercept at 957 ± 17 Ma (Fig. 4). This age is in-
terpreted as the time of the segregation of this
leucocratic material from the older tonalite-
trondhjemite (cf. Luukkonen 1988a). This age
also indicates that the early Proterozoic over-
printing and reheating in the migmatitic tonalites,
even in close proximity to the greenstone belt,
have not been thorough. The lower intercept age
has no apparent relationship to any geological
event, but is high enough to indicate a later
metamorphism.

To the north of the belt occurs cataclastic por-
phyritic-porphyroclastic leucocratic granodiorite,
the typical predominant igneous component of
the late Archaean gneisses in eastern Finland
(Hyppönen 1983; Luukkonen 1985,1988b). The
contacts between the Saari-Kiekki greenstone belt
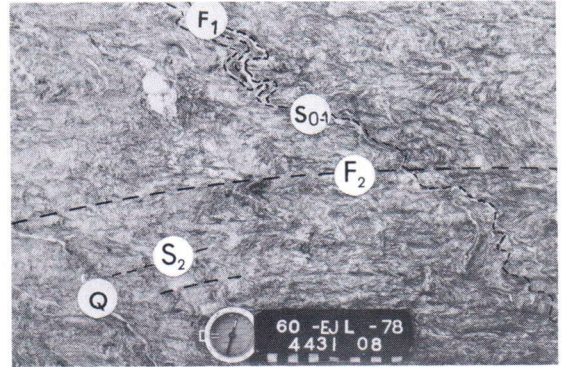and the late Archaean basement are not exposed,

Fig. 5. Blastomylonitic basic volcanite (perhaps tuff/tuffite)
showing early Proterozoic S_o, tight isoclinal F_1 folding with
S_1 foliation, S_{0-1} composite foliation, F_2 overturned and
chevron type folding with axial planar S_2 crenulation. Ear-
ly F_1 »blind quartz» veins (Q).

but on the basis of the ultramylonites observed
along the margins, they are deduced to be tec-
tonic in character (Fig. 5). The total thickness of
the greenstone belt is c. 2000—3000 m, and three
formations have been distinguished within it.
From bottom to top these are (Fig. 6):

a) the Latvalampi Formation, some 500 m thick,
   characterized by breccia-conglomerates with
   arkosic layers in its upper part. This forma-
   tion occurs principally in the western and
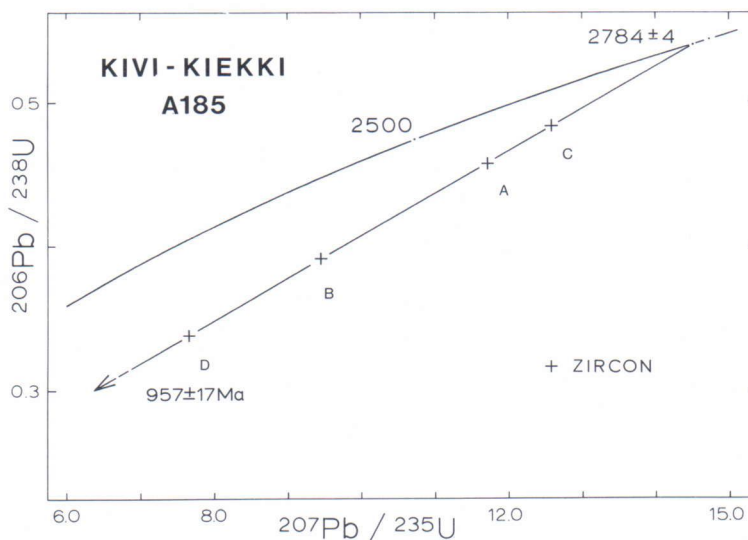   southern marginal zone of the belt.

Fig. 4. U-Pb concordia diagram show-
ing data for leucocratic tonalite from
near the marginal zone of the Saari-
Kiekki greenstone belt. A chord
through 4 zircon fractions has an up-
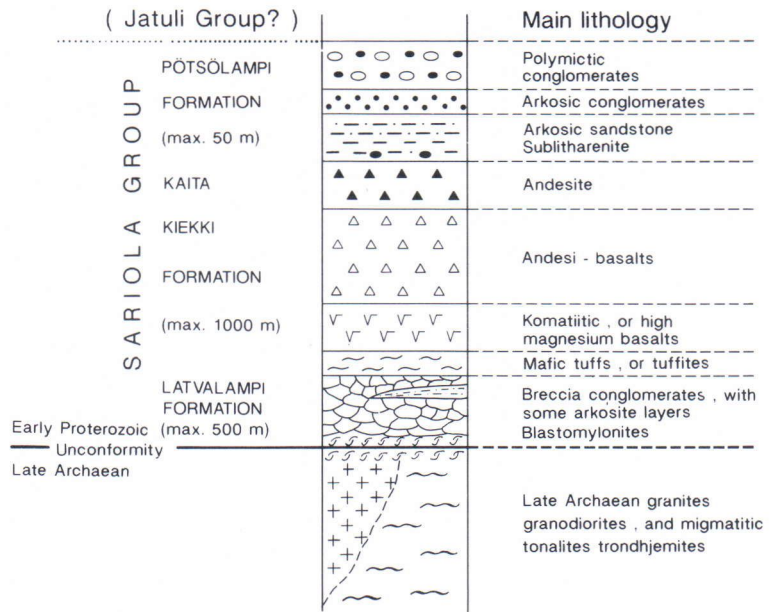per intercept at 2784 ± 4 Ma and a
lower intercept at 957 ± 17 Ma.

Fig. 6. Simplified diagrammatic stratigraphy of the Sariola in the Saari-Kiekki greenstone belt.

b) the Kaita-Kiekki Formation about 1000 m thick and largely composed of basalts, basaltic andesites and/or andesites, which compositionally correspond to komatiites and high magnesium tholeiites, although the indermediate volcanites are calc-alkalic. Structures typical of extrusive rocks are seen in this unit, including varioles, amygdales, agglomerates, breccias and tuffites. The Formation is most extensively developed in the middle and eastern part of the belt.

c) The uppermost unit, the Pötsölampi Formation, is composed of sublitharenites, arkosic sandstones—conglomerates and polymictic conglomerates. The unit varies in thickness from several to tens of metres, and frequently occurs as lenticular, sporadic, isolated formations due to tectonic overthrusting.

All the volcanic and sedimentary rocks described below, have undergone polyphase deformation and low-grade metamorphism. Nevertheless, original volcanic and sedimentary structures are commonly well preserved.

Lithology and age determinations

Although all units in the igneous and sedimentary sequence are metamorphosed, igneous and sedimentary rock names will be used in this paper without the prefix meta.

The Latvalampi Formation

The sedimentary (commonly cataclastic) rocks of the Latvalampi Formation are characterized by the predominance of heterogeneous conglomerate which, due to as angular fragments (Fig. 7) and lack of internal structures is referred as breccia-conglomerate. It is thickest in the western part of the belt, the total thickness being there c. 500 m, and it rests on the late Archaean basement leucotonalites. Near the contacts the formation is cataclastic and mylonitic.

The breccia-conglomerate contains angular, rarely rounded fragments that are representative of the nearby late Archaean basement such as leucotonalite, migmatitic tonalite-trondhjemite, porphyroblastic granodiorite and banded am-
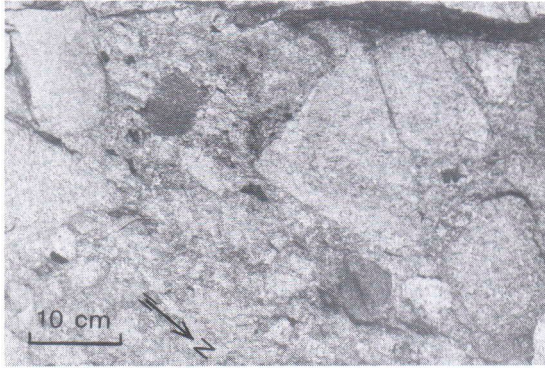
Fig. 7. Clast-supported conglomerate of the Latvalampi Formation.

phibolite, with very little matrix between them. The fragments vary in size from a few tens of centimetres down to granitoid gravel several millimetres in diameter. The granitoid fragments are well preserved whereas the amphibolite ones have completely altered into chlorite or biotite schist. The matrix is an aggregate of sand-sized granitoid clasts, quartz, plagioclase, sericite, biotite, epidote, carbonate and potassium feldspar. The angularity of fragments and the dearth of matrix show that material were transported for only a very short distance.

The zircon population from one angular granodioritic fragment is clear and has an almost euhedral morphology. Four zircon fractions (Table 2, sample A911) from it gives an upper intercept age of 2702 ± 30 Ma (Fig. 8). This age is coeval with the ages of the most prominent late Archaean D_3 granitoid intrusions reported from Kuhmo and Suomussalmi area (cf. Hyppönen 1983; Luukkonen 1988b). The lower intercept with the concordia is 808 ± 63 Ma (Fig. 8), again indicating some later metamorphic event.

In the uppermost part of the Latvalampi Formation there are pinkish, arkosic layers several metres thick which lack primary sedimentary structures. Narrow arkosic »pockets» in the breccia-conglomerate are interpreted to be allochthonous as a result of overthrusting. The material for the arkosic layers is not so local as in the breccia-conglomerate, but it may be from the reworked and weathered late Archaean basement, or in part derived from a chemically altered breccia-conglomerate.

The immature character of the Latvalampi Formation, with material derived from the local basement granitoids, suggests that mechanical erosion dominated over chemical weathering during that time. The Latvalampi breccia-conglomerate probably primarily represents high relief »talus-slope» deposits, implying fault activity,
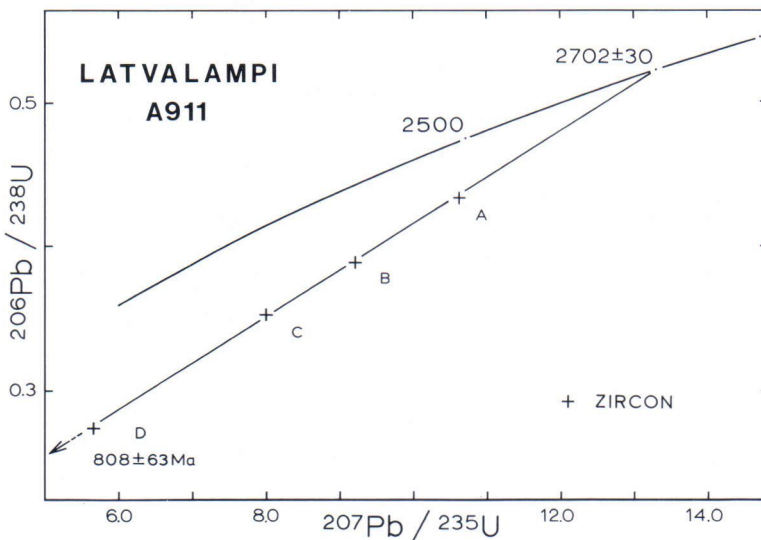

Fig. 8. U-Pb concordia diagram showing data from a granodioritic fragment in the breccia conglomerate of the Latvalampi Formation. A chord through 4 zircon fractions has an upper intercept at 2702 ± 30 Ma and a lower intercept at 808 ± 63 Ma.

where joints and fractures developed in reactivated late Archaean zone of weakness, and promoted mechanical erosion in that rock material. The disaggregated rock material remained in situ, or was transported into topographic lows by solifluxion processes. The presence of arkose »pockets» in the upper part of the formation is evidence of fluvially-reworked, more chemically weathered material in this unit (cf. Miall 1978).

The Kaita-Kiekki Formation

The tuffs or tuffites, and agglomeratic, amygdaloidal, variolitic, massive or brecciated lavas of the Kaita-Kiekki Formation are basic to intermediate in composition (Figs 1,6). In the middle part of the belt, the lowermost unit varies in thickness from a few metres to tens of metres and consists of basic tuffs or tuffites, which are typically cataclastic, dark green, medium to fine grained, and frequently banded (Fig. 9). They contain tremolite—actinolite, chlorite, albite and biotite as the main minerals with carbonate, quartz, epidote, opaque minerals and zircon as accessories. The albite, chlorite and tremolite—actinolite form narrow bands (0.5—2.0 mm thick), while a younger generation of tremolite—actinolite forms large porphyroblasts up to 2.0 mm long parallel to the prevailing S_2 crenulation. Some elliptical albite, quartz—epidote aggregates in tuff/tuffite layers are suggestive of a primary, indistinct lapilli texture (Fig. 9). Thicker bands and/or layering (10—20 cm thick) are due to the varying amount of biotite and tremolite in the darker bands. In more cataclastic, NW—SE-trending zones the rock is chlorite- or quartz-rich and blastomylonites even occur in some places (Fig. 5).

Layered, variolitic, brecciated and massive lavas of komatiitic—high magnesium tholeiitic composition are associated with the unit mentioned above. Major minerals are light coloured amphibole (tremolite—actinolite), chlorite and plagioclase (albite—oligoclase) with accessories including quartz, biotite, epidote, carbonate,
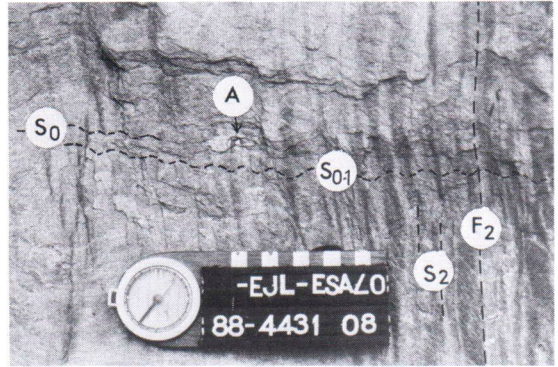
Fig. 9. Banded basic tuff/tuffite of the Kaita-Kiekki Formation showing layering S_0, a composite foliation S_{0-1}, F_2 chevron—kink type folding with axial planar foliation S_2. (A) = indistinct intermediate lapilli in mafic tuff/tuffite.
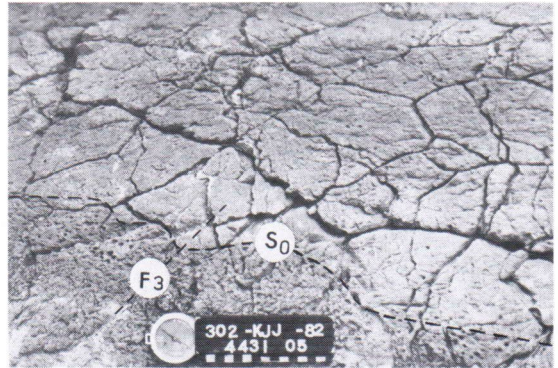
Fig. 10. Brecciated komatiitic—high magnesium basalt of the Kaita-Kiekki Formation showing layering (S_0), dextral F_3 folding, and variolitic structure towards the top of the basaltic lava layer.

opaque and titanite. The original texture has generally been destroyed due to the recrystallization, and plagioclase, for example, is usually recrystallized to a granoblastic mosaic. The variolitic, brecciated structures and layering are very well seen in cross-section perpendicular to the prevailing S_2 foliation (Fig. 10). The variolitic structure is common in the upper part of each layer and a typical feature for this lava unit. The varioles are 1—9 mm in size, elongated in the direction of the main lineation (L_2), and they are composed mainly of granoblastic plagioclase

and quartz, with varying amounts of tremolite and epidote.

The bulk of the Kaita-Kiekki Formation is composed of amygdaloidal, brecciated, almost totally recrystallized basaltic andesite flows, with a few interlayers of andesites that may in fact be tectonic slices. The major minerals are hornblende (or tremolite—actinolite), plagioclase (albite—oligoclase) and quartz. Biotite is present in minor amounts in NW—SE-trending cataclastic zones. Chlorite, opaque minerals, epidote, titanite and zircon are accessory minerals. The original volcanic texture has generally been destroyed with plagioclase and quartz recrystallized to granoblastic mosaic. The amygdules (0.5—3.0 mm in size) are filled with quartz, tremolite and albite and in some places with biotite, and surrounded by a fine grained quartz—plagioclase—tremolite rim. Some of the globular, variolitic textures (1—12 mm in size) in numerous basaltic andesite layers are interpreted to be the result of spherulitic crystallization (Fowler et al. 1987). Varioles are composed of a granoblastic quartz —plagioclase mass, with additional variable amounts of colourless tremolite, epidote and opaque. Radiating crystals of plagioclase, or pyroxene are no longer seen and the present felsic composition of the varioles merely reflects the albitization of the former Ca-rich plagioclase. The polygonal jointed lava layer, in the inner part of the Formation, formed as a consequence of thermal contraction as the lava flow cooled (Fig. 11). The joints, with light coloured rims, separate angular units from a few centimetres to a few tens of centimetres. In this lava unit, indistinct brecciated, variolitic pillow lava has been found on the northern shore of Kaita-Kiekki lake reflecting a probable subaqueous volcanic origin. Close to the NW—SE-trending fault zones, the volcanic rocks have subparallel crenulation (or S_2 schistosities) and are altered into chlorite schists or chlorite-biotite schists and tectonic breccias associated with penetrative metasomatic processes, mainly albitization. Elsewhere such penetrative deformation is difficult to detect.
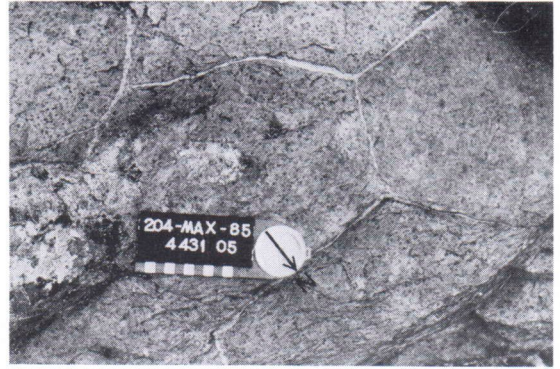

Fig. 11. Pentagonally jointed basaltic andesite of the Kaita-Kiekki Formation. Figure perpendicular to the prevailing lineation (L_2).

The uppermost unit of the Kaita-Kiekki Formation contains amygdaloidal, brecciated and agglomeratic andesites. Distinctive and commonly seen features of this unit are round to ovoid, pale globules generally 4—10 cm in size (Fig. 12) that can be interpreted as the ocellar structure of rapidly cooling immiscible, intermediate and felsic magma (possibly result of crustal contamination cf. p. 174—175). The top of the andesitic layers crystallized rapidly to produce chilled margins, whereas the cooling in the rest of the intermediate magma caused unmixing, producing immiscible droplets of light felsic liquid (ocelli), which rose and coalesced as light globules in more dense, intermediate andesitic lava matrix. The globules are best seen on the outcrops perpendicular to the main lineation (= L_2; Fig. 12) and are now composed of epidote, quartz, albite and colourless amphibole, merely reflecting the albitization and epidotization of the former Ca-rich plagioclase globules. Elsewhere the rock contains varying amounts of quartz, albite, light coloured amphibole and hornblende with accessory epidote, chlorite, biotite, opaque and titanite. The andesites are totally recrystallized, but amygdules, which have also been found in the light globules and agglomeratic structures, are clearly visible. Tectonic breccias associated with the metasomatic albitization, epidotization and
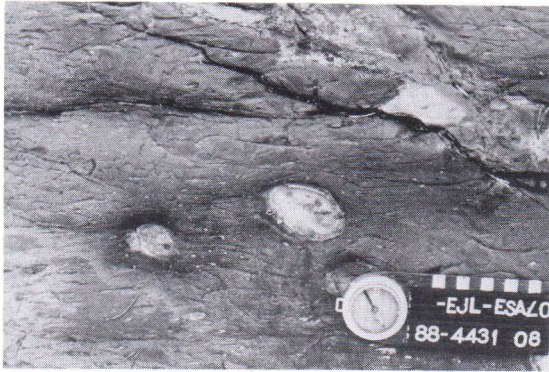
Fig. 12. Andesite lava with elongated pale globules and amygdules of the Kaita-Kiekki Formation. Figure perpendicular to the prevailing lineation (L₂).

Fig. 13. Polygonal jointed, and NW—SE-trending (F₂) metasomatically altered fault zone (A) of the Kaita-Kiekki Formation.

biotitization can be seen close to the NW—SE-trending fault zones in several places (Fig. 13).

All the lava flows of the Kaita-Kiekki Formation show mainly subaereal characteristics, such as breccia, amygdaloidal, pale globules, varioles while subaqueous features are seldom visible. The Formation is interpreted to have been erupted under subaereal or even partly shallow water conditions.

The Pötsölampi Formation

Narrow, tectonically isolated »pockets» of the Pötsölampi Formation form the uppermost unit in the Saari-Kiekki greenstone belt stratigraphy (Figs 1,6). It occurs in the central and southeastern part of the belt, and consists of the sublitharenites, arkosic sandstone—conglomerates and polymictic conglomerates. The maximum observed thickness of the Formation is only a few tens of metres.

In a NW—SE-trending, tectonically isolated basin, near Pötsölampi in the central part of the belt, andesite is overlain by sublitharenite (terminology after Pettijohn 1975) only few metres thick, and composed of approximately 5—10 % subangular, elongated sericite schist fragments, possibly representing of boudinage of discontinuous interbeds of tuffaceous siltstone or claystone in an arkosic sandstone matrix (Fig. 14; the real pelite fragments are met with in nearby glacial erratic boulders). The sublitharenite is overlain by 10—20 metres of arkosic sandstone and is composed mainly of quartz, albite, potassium feldspar and sericite. The accessories are chlorite, biotite, opaque minerals, zircon and rutile. Despite the cataclastic and pseudoclastic texture, the original outlines of sand-sized grains are in places visible under the microscope, and the roundness of these grains is generally poor. The sublitharenite and the arkosic sandstone can be correlated with the sheetflood facies, the overbank facies more typically consisting of fine sands, with thinly interbedded silts and clays (cf. Hempton et al. 1983).

Arkosic sandstone—conglomerate occurs together with the arkosic sandstone and even where very cataclastic, its texture is very well seen in the outcrops perpendicular to the prevailing lineation (Fig.15). It consists of granitoid and feldspar pebbles (1—4 cm in size) eroded from late Archaean granitoids, and some chlorite schist clasts that come from the greenstone belt itself. The matrix is composed of fine grained quartz, feldspar and sericite. The arkosic sandstone—conglomerate is interpreted as sheetflood facies, consisting of horizontally laminated or massive sheets of pebbly sands (cf. Hempton et al. 1983).

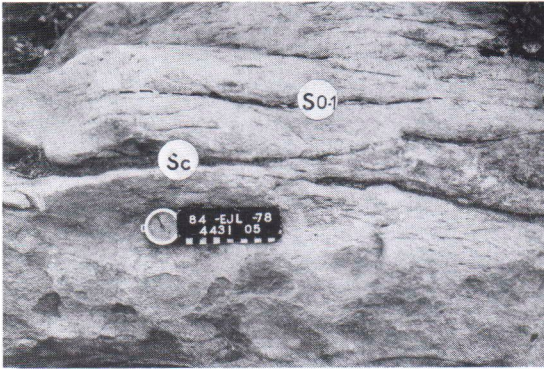The detrital zircon population in the sub-

Fig. 14. Sublitharenite with elongated, boudinaged sericite schist (SC) (parallel to S_{0-1-2}) layers in the Pötsölampi Formation.

Fig. 15. Arkosic sandstone—conglomerate of the Pötsölampi Formation.

litharenites and arkosic sandstone—conglomerate is dominated by fine grained, yellowish and subrounded grains. Ten analyzed fractions (four of which were cleaned by abrasion) form an array (Table 2, samble A912, 913) with an upper intercept on the concordia at 2686 ± 66 Ma and the lower intercept at 238 ± 118 Ma (Fig. 16). This age (within error limits) and the composition of pebbles in the arkosic conglomerate indicate that the main detrital source of the material was the late Archaean D_3 granitoids.

The uppermost suite, coeval with the sublitharenite and arkosic sandstone—conglomerate in the Pötsölampi Formation is commonly a cobble and boulder dominated, volcaniclastic, polymictic conglomerate and a matrix-supported conglomerate has also been found near the Soviet border. The granitoid clasts are more rounded than the clasts of the breccia conglomerates in the Latvalampi Formation. The absence of pyroclastic and lava interbeds indicates that the polymictic conglomerates were deposited after the cessation of volcanism. It occurs as lenticular »pocket» -like allochthonous layers in the greenstone belt, and in the brecciated late Archaean granitoids (Fig. 1). Rounded to subangular boulders, cobbles and pebbles 5—70 cm in size are of late Archaean granitoids, or volcanic
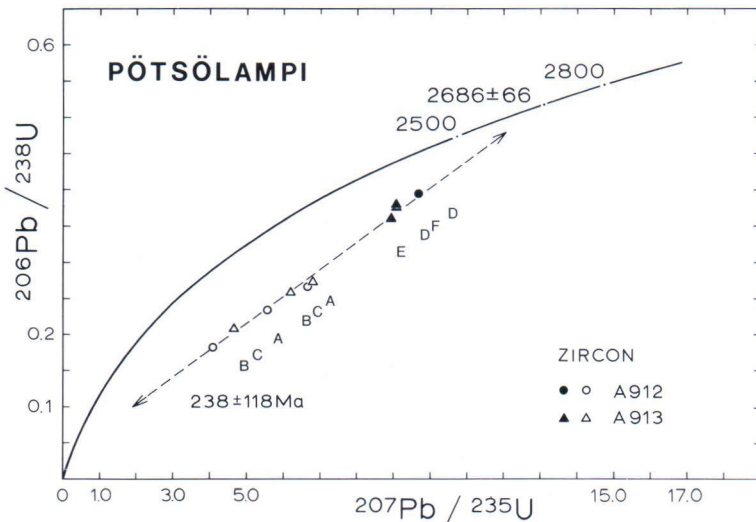

Fig. 16. U-Pb concordia diagram showing data for detrital zircons from sublitharenites and the arkosic sandstone—conglomerate of the Pötsölampi Formation. A chord through 10 zircon fractions has an upper intercept at 2686 ± 66 Ma and a lower intercept at at 238 ± 118 Ma. Abraded fractions marked with filled circles and triangles.

lithologies from the lower part of the greenstone belt (Figs 17, 18), and also quartz porphyry pebbles from an unknown source have been found near the Soviet border. The matrix is rich in chlorite and amphibole, and in places granitoid and feldspar gravelly detritus is abundant. The polymictic conglomerate commonly lacks primary internal texture and is poor in matrix. Accordingly it is fluvially-reworked, with clast supported conglomerate being typical deposits in the margins of fault bounded basins (Hempton et al. 1983).

One granitoid boulder of the polymictic conglomerate has been dated. The interpretation of an isotope system consisting of five isotope ratios for zircons from Sample A186 Saari-Kiekki (Table 2), is somewhat unambiguous. The most probable solution is a chord through points A,B,C which has an upper intercept at 2683 ± 40 Ma (Fig. 19), being almost coeval (within error limits) with the late Archaean D_3 granitoids. All three isotope ratios for titanites lie above the concordia showing an age approximately 1800 Ma (Fig. 19). The corresponding $^{207}Pb/^{206}Pb$ ages are 1858, 1850 and 1794 Ma. This result is quite significant, because Proterozoic ages for titanites have not been found in the Archaean formations in Kuhmo—Suomussalmi area, and may indicate

Fig. 17. Granitoid-volcaniclastic clast-supported conglomerate of the Pötsölampi Formation.

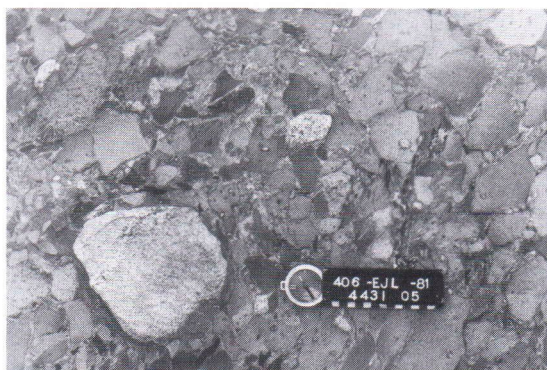
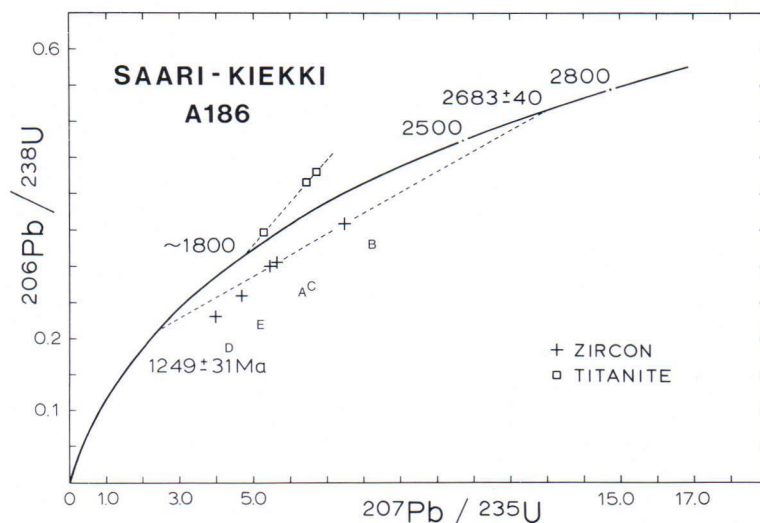Fig. 18. Volcaniclastic clast-supported conglomerate of the Pötsölampi Formation.

Fig. 19. U-Pb concordia diagram showing data for a granitoid boulder from polymictic conglomerate of the Pötsölampi Formation. A chord through three zircon fractions has an upper intercept at 2683 ± 40 Ma and a lower intercept at 1249 ± 31 Ma. A chord through three titanite fractions gave an age of c. 1800 Ma.

local metamorphic resetting during the Sveco-fennian orogeny in the Saari-Kiekki greenstone belt.

The pebble population of the arkosic sandstone conglomerates and the cobbles and pebbles in the polymictic conglomerate as well as the composition of the sandstone in the Pötsölampi Formation indicate a mixed provenance of both the Kaita-Kiekki-type volcanic rocks and the late Archaean granitoids. It also provides evidence for recycling of the older Latvalampi Formation into overlying stratigraphic units in the terrigenous sedimentary succession. The major element geochemistry of the sublitharenites and arkosic sandstones—conglomerates show a low to moderate maturity (Table 1). The chemical index of alteration (CIA) of Nesbitt & Young (1982) ranges from 66.14—68.59 and the major element composition of the sublitharenites and the sandstones, as well as the age determinations from the detrital zircons of the Pötsölampi Formation, suggest that the late Archaean D_3 leucotonalites, granodiorites and tonalites dominated in the source area.

Diabase dykes

Varially undeformed, diabase dykes several tens of metres thick, trending NW or NNW across the Saari-Kiekki greenstone belt and the surrounding late Archaean granitoids are the youngest rocks in the area. Hornblende and andesine are the predominant minerals, but clinopyroxene, orthopyroxene and andesine are the main minerals in the southeast corner of the study area. Leucoxene, magnetite, quartz, biotite, chlorite, titanite and zircon occur in minor proportions. Light coloured, albite-rich, roundish segregations 20—50 cm in size have been found in the dykes north of the Levävaara hill. Despite recrystallization, the primary ophitic texture is clearly visible as a blasto-ophitic texture in the majority of the dykes studied.

The zircon population of the albite-rich segregations in the Rasiaho diabase dyke (Fig. 1; sample A261) contains three different type of zircons,

the majority of which are obscure, redbrown and short. The 3.8—4.0 g/cm^3 fraction includes normal magmatic, euhedral, translucent zircons (found as cores within the prevailing red-brown zircon crystals) and half of the 4.3—4.6 g/cm^3 fraction contains platelike, yellowgreen grains (Table 2, sample A261). However, the U—Pb data for two titanite fractions (Table 2; sample A261) are more concordant than for the zircon fractions. The proper age 2209 ± 11 Ma is based on them, being the mean value for both the titanite fractions (fractions K and J), and the limits of error ± 11 Ma is the deviation in both directions. This age is interpreted as the time of crystallization of the diabase dykes, which is coeval with the diabase dykes in nearby map sheet areas (cf. Hyppönen 1983). U-Pb data for the translucent zircons (fractions I and L), and for two titanite fractions defines a chord which gives an upper intercept with the concordia at 2224 ± 30 Ma, and a lower intercept at 568 ± 298 Ma. This regression is indicated by the dotted line in the concordia diagram of Fig. 20.

Geochemistry and petrogenesis of the volcanites

The Saari-Kiekki greenstone belt has a low metamorphic grade and the initial designation of different rock types was aided by geochemistry. However, it has been shown that in the NW—SE-trending early Proterozoic structural zones, alteration processes such as hydration, carbonatization, albitization, and epidotization, if extensive, will, drastically alter the primary chemical composition of the rock. The best analyses were used in the definiting of three classes; basalts, basaltic andesites and andesites. Classification into the other units of the Formation was based largely on overall field appearance, texture and petrology together with the geochemical characteristics. All the analyses of major and minor elements in this study, given in Table 1, were carried out at the Research Laboratories of Rautaruukki Co. using XRF techniques.
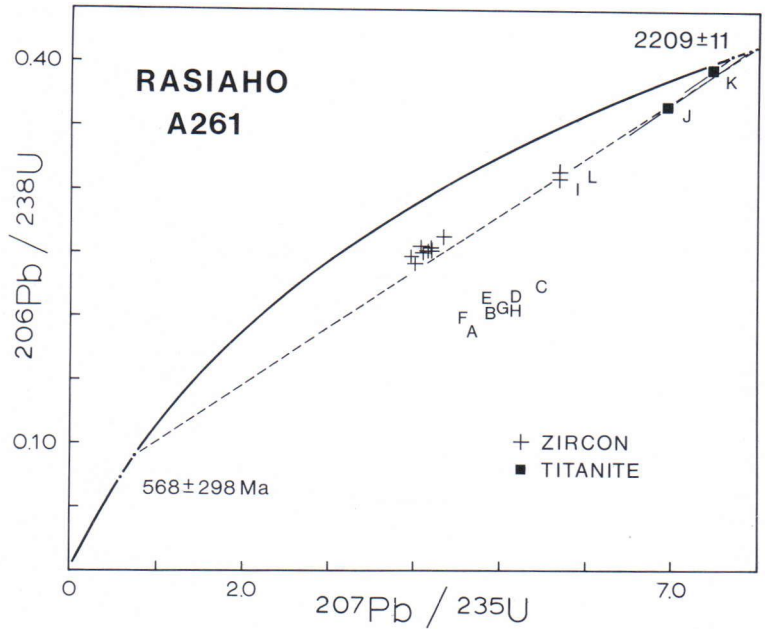
Fig. 20. U-Pb concordia diagram showing data for the Rasiaho diabase dyke (the albite-rich segregations). A chord through two titanite fractions gives an age of 2209 ± 11 Ma (= solid line). A chord through two zircon (translucent) and two titanite fractions has an upper intercept at 2224 ± 30 Ma and a lower intercept at 568 ± 298 Ma (dotted line).

According to the classification of Irvine & Baragar (1971) the volcanites of the Kaita-Kiekki Formation would be located in the tholeiitic and calc—alkalic fields in the AFM diagram. The great majority of the analyses fall in the calc—alkalic field being basaltic andesites and andesites. Only basic tuffs and some of the lowermost basalts in the Kaita-Kiekki Formation are tholeiitic (Fig. 21). All the early Proterozoic diabase analyses form a distinct group in the iron-rich tholeiitic field, as do most of the early Proterozoic diabases in nearby map sheet areas (Kilpelä 1990).

The MgO-CaO-Al$_2$O$_3$ diagram shows that the basic volcanites cluster into two groups, the komatiitic—Mg-rich tholeiitic basalts and the normal tholeiitic basalts (Fig. 22). For the komatiitic—high magnesium basalts MgO contents are 7.55—11.0 %, and Al$_2$O$_3$ contents 10.30 —13.40, being thus more aluminium-rich than typical Archaean Barberton-type komatiitic basalts (Viljoen et al. 1982). A very clear compositional break emerges between the two main basaltic groups. MgO content for the latter, the normal tholeiites, is between 3.76—8.67 %. The analyses

showing the existence of an aluminium-rich trend, are interpreted to be derived from altered rocks, epidotized and albitized basalts, basaltic andesites and andesites.

The compositional break between the two basic volcanite types is also seen on the Jensen (1976) diagram (Fig. 23). On the original Jensen diagram the line separating the tholeiite from the komatiite field transects the other group of basic volcanites. Only the six most basic analyses (from basic tuffs/tuffites and lower basic lava) are real komatiitic basalts, and the remainder being magnesium-rich tholeiitic basalts, or calc-alkalic basalts—basaltic andesites. The anomalous high Al$_2$O$_3$ contents in five basaltic andesites are obtained from the altered, albitized and epidotized rocks, in NW—SE-trending faults. Two analyses of the younger diabases plot in the tholeiite field as in AFM diagram.

In terms of the criteria applied to classify modern orogenic andesites published by Gill (1981), the basaltic andesites and the andesites in the Saari-Kiekki greenstone belt resemble a typical mantle derived, low-potassium, calc—alkalic fractionation trend (Fig. 24). Since the calc-alkalic
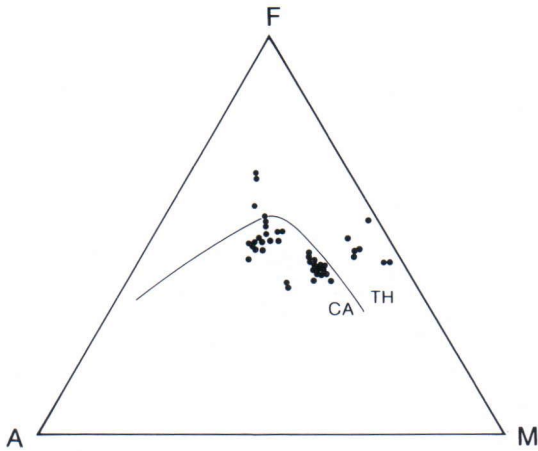
Fig. 21. AFM diagram for volcanites from the Kaita-Kiekki Formation. Heavy solid line separates tholeiitic (TH) from calc-alkaline (CA) suites using the criteria of Irvine and Baragar (1971).
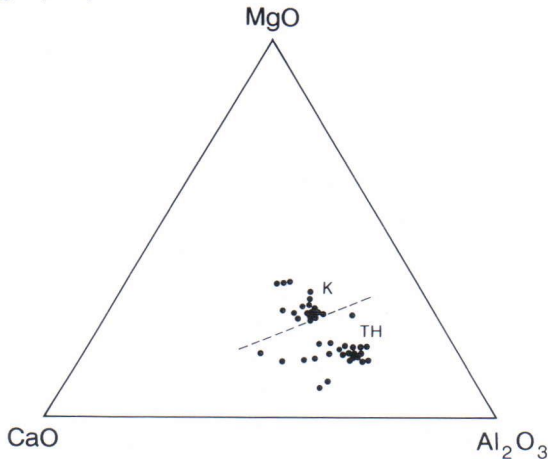
Fig. 22. CaO-MgO-Al$_2$O$_3$ diagram showing compositions of komatiitic (K) and tholeiitic (TH) lavas of Kaita-Kiekki Formation.
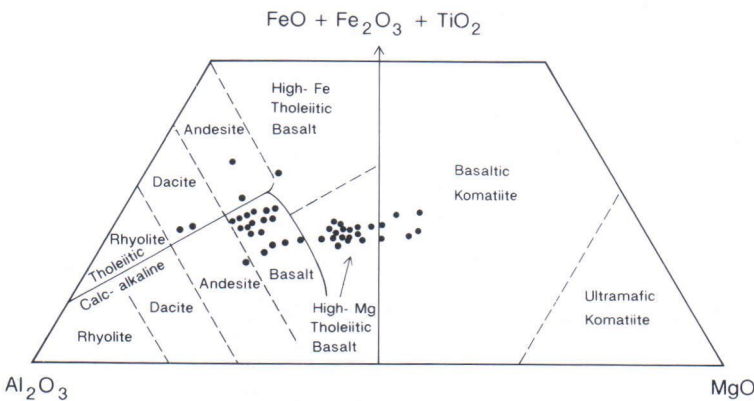
andesites typically predominate near convergent plate margins, the explanation for the origin of Saari-Kiekki andesites must be exceptional as they are associated with strike-slip faulting in the late Archaean craton. The major-element compositions of continental flood basalts (= CFB) and mafic dykes world wide indicate that very few mantle-derived CFB magmas have reached the surface without pausing and re-equilibrating during their ascent through the crust, particularly in the case of post-Archaean basalts (Thompson et al. 1983; Condie 1985). In the area studied the brecciated late Archaean migmatites and granitoids in the crust could easily have been partially fused during the ascent of hot komatiitic—high magnesian basaltic magma, and crustal contamination is quite plausible. When the komatiitic—high magnesian magmatism was initiated, the crust was cold enough to allow some basalts to penetrate to the surface (= lower basic tuffs/tuffites and basic lava in the Kaita-Kiekki Formation). Simultaneously basaltic extrusions added heat to the tonalitic (-granodioritic) crust, and partial melting as well as stronger crustal contamination was possible. However, the crust in Saari-Kiekki area evidently did not become sufficiently hot and ductile as to result in the generation of felsic magma. Thus instead of rhyolites and granites, the Saari-Kiekki sequence contains basaltic differentiates and/or hybrid basaltic andesites—andesites (basalt + crust) (cf. Huppert et al. 1984; Huppert and Sparks 1985, 1988). For example if the basalt contained 48%

Fig. 23. Jensen cation diagram showing the distribution of volcanic rocks from the Kaita-Kiekki Formation. Fields divided after Jensen (1976).

SiO_2 before contamination it would be basaltic andesite or andesite after contamination by the tonalitic crustal material in the Saari-Kiekki area (cf. Pearce 1983). The crustal contamination of basaltic material at depth during the uprise of magma could explain the high proportion of basaltic andesites and andesites in the Kaita-Kiekki Formation. According to Huppert and Sparks (1985) thermal erosion during the ascent takes place on both sides of the feeder dyke, and under some circumstances, the amount of crustal contamination may reach 30—40 %. The evidence for this kind of phenomenon can be demonstrated by $Zr/Mg^{\#}$ ($Mg^{\#} = Mg/(Fe_{tot} + Mg)$) ratios being above the fractionation trend, and correspondingly $V/Mg^{\#}$ ratios being below the fractionation trend (Fig. 25), since Zr tends to be enriched in continental crust whereas V is relatively depleted. In the case of volcanites in the Kaita-Kiekki Formation, the parental magma (= lowermost komatiitic basalt) is close to average komatiite in composition. Therefore the data in the Figure 25 possibly indicate the effects of significant custal contamination. However, the absence of REE and isotopic data limit the confidence of this assertion.

Structural history

In the late Archaean basement away from the Saari-Kiekki greenstone belt, early Proterozoic reactivation has been resolved mainly as a brittle shearing along the E—W, NW—SE and NE—SW-trending late Archaean zones of weakness (cf. Luukkonen 1985, 1988a,b). Elsewhere all the late Archaean structural patterns are very well preserved, even in the vicinity of the marginal zones of the Saari-Kiekki greenstone belt. The marginal faults of the belt are part of a pattern of late Archaean dextral faults (D_4 and D_5), which were again active during the early Proterozoic Sariolan and Jatulian time.

Fig. 24. Classification of basaltic andesites (filled symbols) and andesites (open symbols) of the Kaita-Kiekki Formation using major-element criteria developed for modern orogenic andesites (Gill 1981).
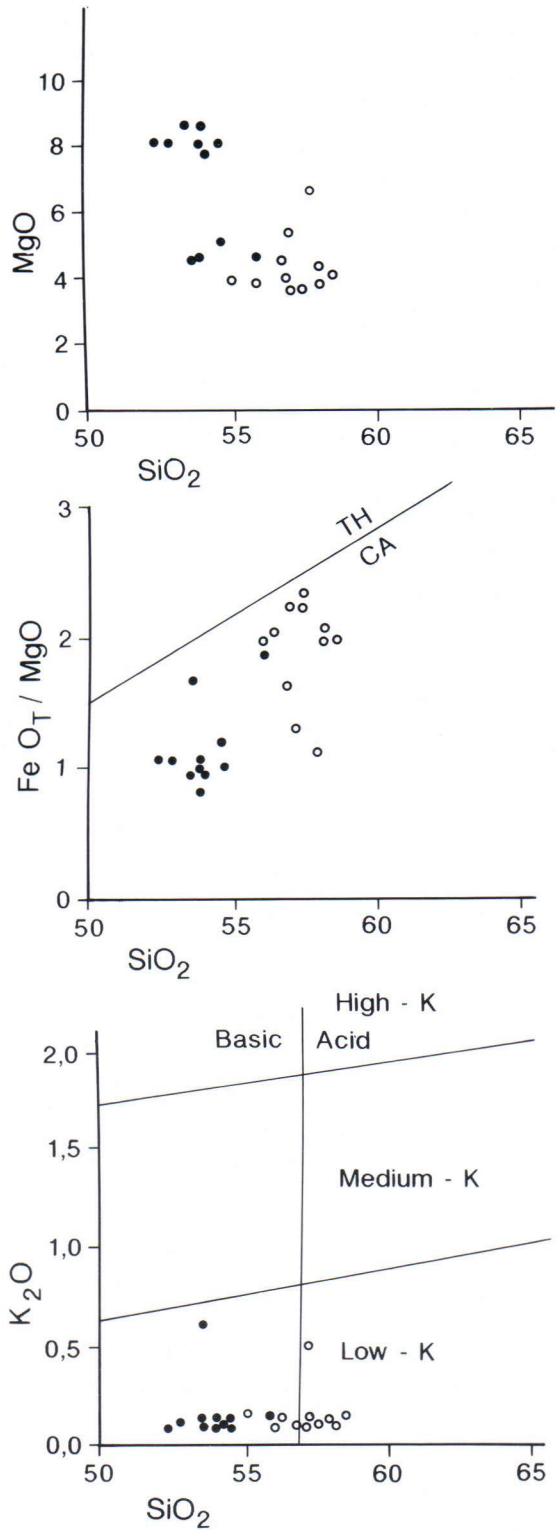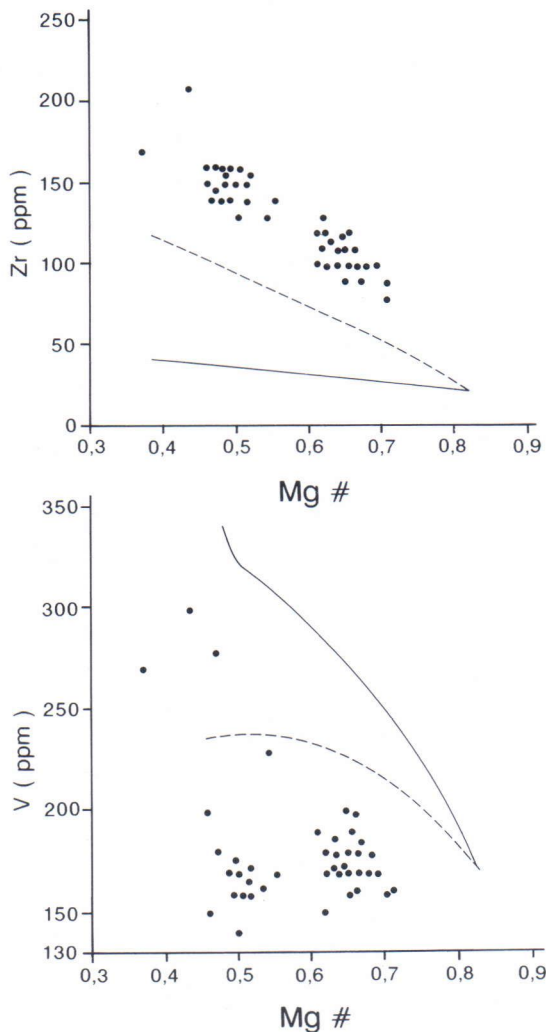
Fig. 25. Zr and V against magnesium number (Mg # = Mg/(Fe$_{tot}$ + Mg)) variation diagrams. Solid lines represent fractional crystallization trends from the average komatiitic composition, and dashed lines represent assimilation-fractional crystallization trends calculated using the composition of modern upper crust (Taylor and McLennan 1981), contamination/crystallization ratio of 0.4 was used according to the criteria of Arndt and Jenner 1986.

Within the belt, the cataclastic zones, the narrow volcano-sedimentary layers beneath the lava flows of the Kaita-Kiekki Formation, and the sedimentary rocks of the Latvalampi and Pötsölampi Formations tend to be areas of major movement and thus represent zones of intense and heterogenous strain, resulting from localized discrete structural events during early Proterozoic time.

First deformational phase (D$_1$)

Only in a few outcrops it is possible demonstrate that S$_1$ is subparallel to S$_0$ (Figs. 5, 9). S$_1$ varies in intensity from a relatively weak mineral growth in interiors of the Kaita-Kiekki lava layers to a transposing mylonitic foliation in sedimentary rocks. Folds of the first deformational phase, which are tight to isoclinal with gently to moderately plunging E- or W-trending fold axes and a moderately dipping axial plane, are well preserved in basic tuffs/tuffites and sublitharenites. Peculiar to and typical of the early stage of intensive F$_1$ deformation are »blind» quartz injections a few millimetres thick in the mafic tuffs/tuffites (Fig. 5). The mylonitic features of S$_1$ are interpreted as evidence for early gliding in these rock horizons.

Second deformational phase (D$_2$)

F$_2$ folding comprises open to tight, dextral, overturned folds that deform S$_0$ and S$_1$. F$_2$ fold axes vary from horizontal to steeply inclined and plunge either W—NW or E—SE. Unlike structures of the earlier deformational phase, the products of the second deformational phase are prominent almost every outcrop; reorientation of earlier structures is frequently seen. Faults with dextral displacement are also common, generally parallel to F$_2$ axial planes, and containing cataclasite and blastomylonite.

Basin-fill thickness is asymmetric with respect to D$_2$ overthrusting, with maximum thickness developed adjacent to the southeastern margins of the major NW—SE faults, and decreasing towards the northwest (cf. Fig. 1, 26). This accounts for the volcanic and sedimentary rocks comprising stacked sequences, lying at a low angle with intraformational unconformities (= »pocket»-like). Similar structural features are found in the Sumi-Sariola Formations of the
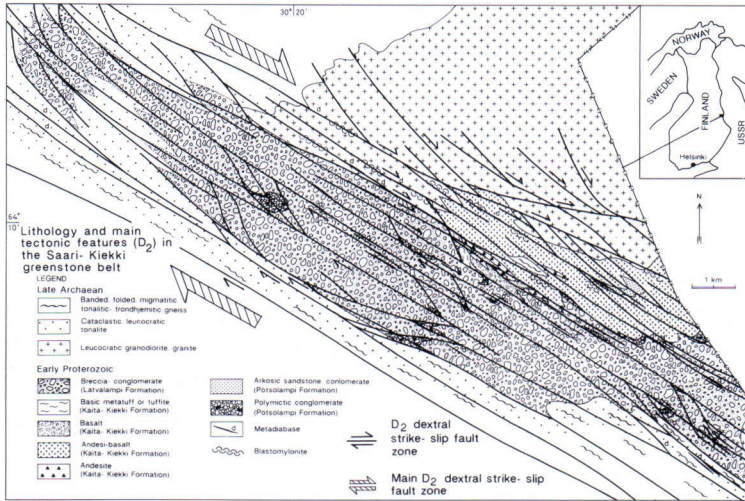
Fig. 26. Main D_2 dextral strike-slip faults in the study area studied as seen in the field and from topographic maps. Lithologies as in Fig. 1.

Shombozero area in Soviet Karelia (cf. Zhuravlev et al. 1979).

A strong axial planar S_2 foliation cuts across S_0 and S_1. It is developed particularly well in the sedimentary rocks of the Kaita-Kiekki and the Pötsölampi Formations. In many places it is shown by the strong preferred orientation of chlorite, tremolite—actinolite, albite and quartz, which post-dates the D_1 amphibole, tremolite and oligoclase. In the other rock units S_2 is more widely spaced. A strong mineral lineation (L_2) is expressed by elongate chlorite, younger tremolite and biotite crystal aggregates. The presence of the biotite means that the metamorphism reached the epidote-amphibolite facies PT -conditions during early-D_2, and was accompanied by hydration, carbonization, epidotization, albitization and potassium metasomatism in the vicinity of NW—SE-trending fault zones. Increased carbonate and potassium metasomatism resulted in breakdown of Ca-plagioclase and amphibole, and an increasing proportion of chlorite, quartz, albite, calcite and biotite, hence causing incoherent trends in variation diagrams (Figs 21,22,23) and high Al_2O_3, CaO and SiO_2. Metamorphism declined to greenschist facies towards

the end of the structural evolution and homogeneous ductile strain was replaced by the late inhomogeneous brittle strain. The L_2 lineation is defined by the elongation of amygdules and varioles in lava flows of the Kaita-Kiekki Formation and the elongation of pebbles in the polymictic conglomerates of the Pötsölampi Formation. Other features commonly associated with D_2 are blastomylonites, cataclasites and tectonic breccias developed along the D_2 dextral fault zones (Fig. 26). These zones may extend from a few centimetres to tens of metres. The most important fault can be traced to the northwest of the studied area as fault zones, zones of weakness or as a lineament for 120 km or more, and commonly shows late Archaean + early Proterozoic lateral displacement of more than 500 metres in places. The NW—SE-trending diabase dykes show little marginal modification or displacement across the Saari-Kiekki greenstone belt and are interpreted to have been intruded during the later stages of this D_2 early Proterozoic deformation.

Third deformational phase (D_3)

Open, commonly symmetrical gently plunging F_3 folds have almost vertical E—W-trending

4

axial planes and are only seen to deform earlier structures in outcrops of the mafic tuffs/tuffites. Axial planar fabric is weakly expressed, seen only under the microscope as a parallel orientation of youngest chlorite and sericite.

All three deformational phases noticed in the rocks of the Saari-Kiekki greenstone belt could represent the main stages of dextral, early Proterozoic, NW—SE-trending, parallel strike-slip faults and simple shear along reactivated late Archaean zones of weakness.

Conclusion

In the Saari-Kiekki area the structures observed in the greenstone belt deform the late Archaean structures, but the greenstone belt itself is cut by the early Proterozoic (c. 2209 ± 11 Ma) Jatulian diabase dykes (Fig.1). Furthermore the lithological similarity to the other Sumi-Sariola Formations in Soviet Karelia, and the Sariola in Central Finland invites correlation with the Saari-Kiekki greenstone belt (cf. Pekkarinen 1979; Marmo 1986; Strand 1988). However, the absence of radiometric age determinations from the volcanic rocks in the area studied makes it difficult to estimate precisely the age of the Saari-Kiekki greenstone belt. The 2455 ± 5 Ma zircon ages for the quartz porphyry dykes of the Sumi-Sariola Formations in Soviet Karelia (Kratz et al. 1976), 2436 ± 5 Ma zircon age for the large basic—ultrabasic layered intrusions in Koillismaa (Alapieti 1982) and 2435 ± 12 Ma zircon age for the granite porphyry dykes in Moisiovaara area (Luukkonen 1988b), are perhaps correlative with the age of the Saari-Kiekki greenstone belt. Its emplacement is an indication of the same phase of continental rifting and coeval strike-slip faulting associated with the break-up of the late Archaean craton (cf. Park et al. 1984).

The immature character of the sediments in the Latvalampi Formation and restricted deposition of breccias and conglomerates, in an elongate,

fault-bounded basin indicates increased uplift and rapidly subsiding fault zones, as well as the composition of clasts derived locally from the late Archaean basement rocks, suggests that rapid mechanical erosion surpassed chemical weathering during that time.The presence of arkose layers in the upper part of the Formation gives evidence of a fluvial origin for this unit. The absence of internal sedimentary features in the proximal part of the Formation, probably reflect high topographic relief and fault activity prior to and subsequent to their deposition.

The primary volcanic structures and the composition of the Kaita-Kiekki Formation indicates that they were mainly deposited under subaereal conditions. The composition of the volcanites indicate that they were mantle derived and probably contaminated by crustal material during the underplating before magma ascent if not during their ascent through late Archaean crust. Subsequent autometasomatism during volcanic eruption, and metasomatic processes during D_2 early Proterozoic deformational phase have in places extensively altered their composition.

The composition of the Pötsölampi Formation indicates provenance from the late Archaean basement, from the recycled Latvalampi Formation and from the volcanites of the Kaita-Kiekki Formation. Tectonic reactivation resulted in vertical movements during which older and already chemically weathered crust was eroded and redeposited. In places the debris was sorted into mature sands and gravels, perhaps by braided rivers as now recorded by the sublitharenites, arkosic sands—sandstones and polymictic conglomerates. Clast composition and age determinations from the arenites and polymictic conglomerates of the Pötsölampi Formation indicate that late Archaean leucotonalites, granodiorites and tonalites were dominant at the erosion level of the study area during deposition.

Prior to the first deformation in the Saari-Kiekki area there was a combination of early Proterozoic E—W-trending transcurrence and extension (=transtension) in the dextral strike-slip
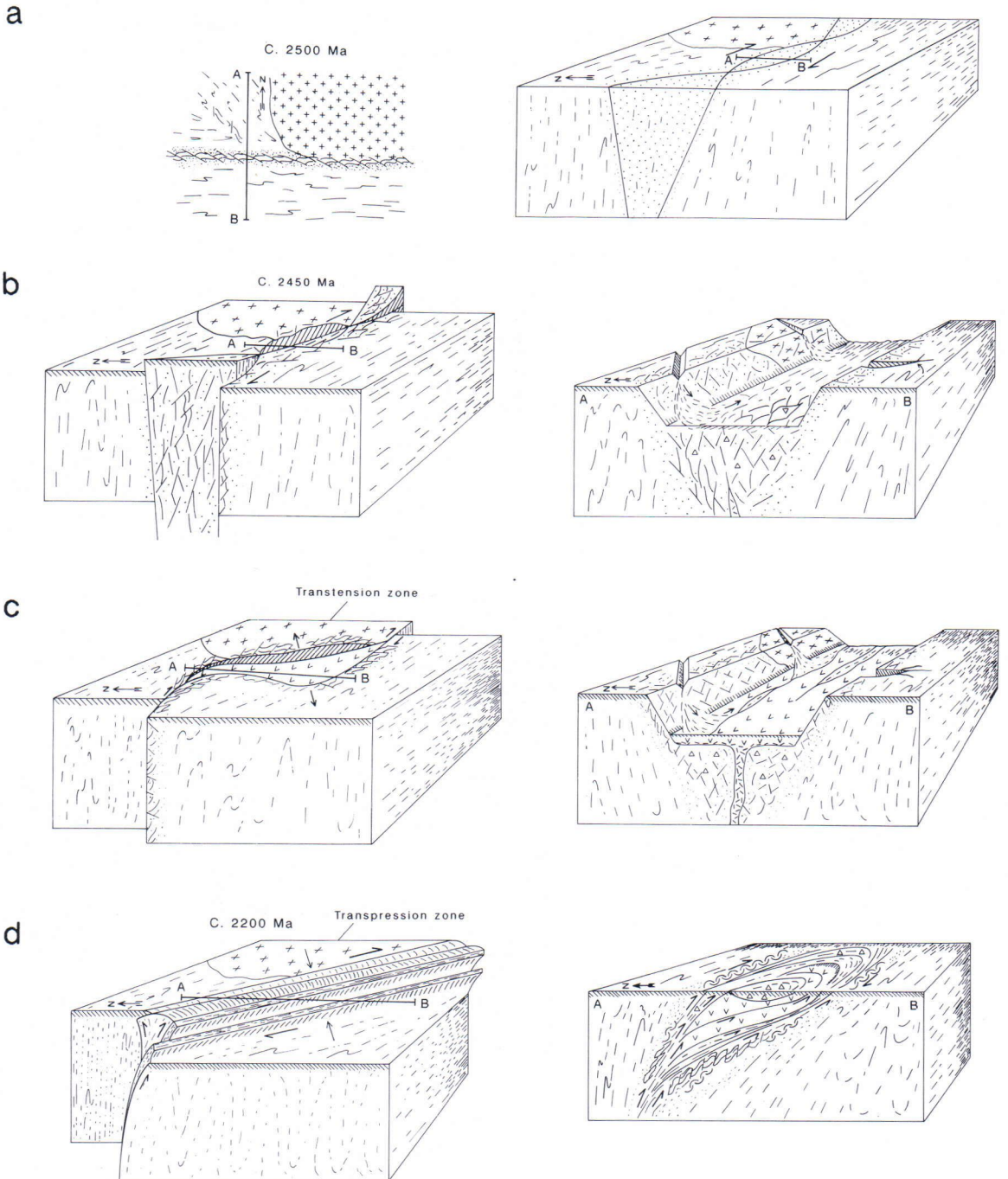
Fig. 27. Schematic models for the four main stages of deformation and deposition during Sariola time in the Saari-Kiekki area. a) Earliest Proterozoic reactivation c. 2500—2450 Ma following late Archaean polyphase deformation; divergent and convergent fault patterns; incipient strike-slip zone. Compare with map in Fig.1. b) Stage of transtension; deposition of the Latvalampi Formation, and initial ascent mafic magma through the crust. c) Continuing extension; deposition of the Kaita-Kiekki and the Pötsölampi Formations. d) Stage of transpression; overthrusting and evolution of the flower structure c. 2200 Ma.

fault zone. When the dextral, E—W-trending strike-slip movement contains the same sense of shear as that of the main fault, it leads to extension of the sector, stratal thinning and the development of normal fault systems obliquely inclined (= NW—SE trend) to the strike of the main fault. This reactivated both the E—W and NW—SE-trending late Archaean (D_5 and D_4) zone of weakness (Fig. 27a), which together give alternate zones of divergence and convergence and are formed within continental crust. At first the extension was limited, causing »small sag ponds» along the strike-slip fault. The deposition of breccias and conglomerates of the Latvalampi Formation at the basin margins represents talus detritus or alluvial fans (Fig. 27b). As extension proceeded, crustal thinning allowed magma to rise and basalts, basaltic andesites and andesites of the Kaita-Kiekki Formation extruded. The latter part of the evolution of the Saari-Kiekki greenstone belt is typified by various mass gravity transport processes. Redeposition of the earlier material commenced, with the stratified sediments and the conglomerates of the Pötsölampi Formation and breccias continued to form at the faulted margins (Fig. 27c).

The first and second deformational phases in the structural history are marked by transpressive regimes: strike-slip faulting of E—W and NW—SE trend, overthrusting, folding and uplift. In the NW—SE-trending strike-slip fault (= in the reactivated late Archaean D_4 zone of weakness), the strong transpression lead to the tectonic extrusion of the Saari-Kiekki greenstone belt, resulting in a series of convex upward reversed, or thrust faults, forming a structure better known as a flower — or palm tree-structure

(Fig. 27d; cf. Harding 1985, Ramsay and Huber 1987, Sylvester 1988). The present Saari-Kiekki greenstone belt is interpreted as an eroded, early Proterozoic positive flower structure. The later stage of D_2 leads in places to the intrusion of NW—SE-trending Jatulian (2209 ± 11Ma) diabase dykes and the D_3 in the structural history possibly represents the latest stage of this transpression.

The late Archaean reactivated zones of weakness in the Saari-Kiekki area have changed from a transtensile regime in the Sariolan time to a transpressive one in the Jatulian time and caused »stratal shingling» which is younging towards the depocenter. This type of the change from one regime to another is also typical for younger strike-slip fault systems (Nardin & Henyey 1978; Carter & Norris 1976; Norris et al.,1978; Reading 1980; Hempton et al. 1983), and seen as well in the much more extensive Sumi-Sariola Formations of Soviet Karelia (cf. Zhuralev et al. 1979).

As a whole the reactivated late Archaean zone of weakness has been both the depocenter for Sariolan sediments and volcanites, and later on, where the volcano-sedimentary succession was preserved from subsequent erosion (= »pocket»-like formations in the reactivated late Archaean fault zone).

Table 1. Chemical analyses of volcanic and sedimentary rocks from the Kaita-Kiekki and Pötsölampi Formations: 1—40 *Kaita-Kiekki Formation,* 1—4. Mafic tuff/tuffite, 5—16. Komatiitic—high magnesium basalt, 17—28. Basaltic andesite and 29—40. Andesite; 41—43. Jatulian diabase dyke; 44—46 *Pötsölampi formation,* 44. Sublitharenite, 45. Arkosoc sandstone and 46. Arkosic sandstone — conglomerate.

	1	2	3	4	5	6	7	8	9	10	11	12	13
SiO_2	55.10	49.70	46.90	48.00	51.20	48.10	51.90	49.00	44.90	52.90	54.50	57.70	53.90
TiO_2	0.44	0.47	0.60	0.50	0.48	0.48	0.50	0.58	0.47	0.44	0.51	0.49	0.46
Al_2O_3	10.40	14.30	14.40	14.60	12.40	10.30	13.50	18.70	12.00	16.70	12.90	15.00	12.30
$Fe_2O_{3\,tot}$	9.47	10.07	11.02	10.92	9.71	12.80	9.99	9.81	12.98	7.87	9.08	7.20	9.66
MnO	0.22	0.16	0.17	0.25	0.18	0.23	0.19	0.13	0.27	0.16	0.16	0.12	0.17
MgO	10.30	8.74	9.48	8.67	9.95	11.00	8.25	2.56	10.80	5.67	7.55	5.27	8.30
CaO	8.10	10.30	10.70	10.10	7.51	9.74	8.46	11.40	10.70	11.60	11.20	10.90	10.20
Na_2O	0.41	0.95	1.03	1.48	2.72	1.96	3.56	3.50	1.06	1.00	0.47	0.63	0.63
K_2O	0.09	0.62	0.69	0.16	1.29	0.14	0.08	0.17	0.43	0.23	0.14	0.13	0.20
P_2O_5	0.07	0.13	0.09	0.10	0.10	0.09	0.10	0.14	0.06	0.19	0.09	0.12	0.09
L.O.I.	0.14	1.07	0.74	0.87	0.68	0.38	0.25	0.84	1.10	0.64	0.62	0.43	0.69
Total	94.90	95.70	95.30	95.00	95.70	95.00	96.80	96.10	93.80	96.90	96.80	97.90	96.10
V (ppm)	160	180	200	200	170	180	190	270	200	150	170	170	170
Cr	1140	640	680	610	800	630	620	20	540	500	540	570	550
Cu	90	10	10	10	40	200	40	130	10	150	90	230	10
Zn	100	70	80	310	60	130	100	120	120	70	110	80	110
Ni	240	180	200	180	230	210	180	50	210	110	170	130	160
S	210	230	150	280	200	150	370	530	210	510	430	1600	180
Ba	40	270	290	30	290	30	20	70	190	70	20	20	40
Sr	170	290	250	270	150	60	100	460	60	280	300	380	210
Zr	90	120	120	110	100	90	100	170	80	110	110	120	100

1 = 86-B-78, 2 = 336-A-81, 3 = 336-B-81, 4 = 353-A-87, 5 = 272-C-80, 6 = 87-B-78, 7 = 269-A-80, 8 = 358-B-81, 9 = 356-A-87, 10 = 356-B-87, 11 = 356-C-87, 12 = 356-D-87, 13 = 356-E-87

	14	15	16	17	18	19	20	21	22	23	24	25	26
SiO_2	50.90	51.90	51.20	53.80	52.30	54.60	54.60	52.90	54.10	54.00	54.00	55.90	53.60
TiO_2	0.51	0.47	1.37	0.41	0.50	0.51	0.42	0.47	0.50	0.47	0.62	0.64	0.66
Al_2O_3	12.80	13.90	15.10	10.30	13.40	12.00	17.20	13.30	13.40	11.40	15.50	14.40	16.00
$Fe_2O_{3\,tot}$	10.73	10.44	13.73	9.96	9.61	9.10	6.91	9.61	8.45	9.66	12.16	9.80	8.57
MnO	0.20	0.20	0.23	0.23	0.19	0.12	0.13	0.18	0.16	0.21	0.21	0.15	0.18
MgO	9.42	7.91	2.54	10.70	8.08	8.01	5.08	8.09	7.83	8.56	4.60	4.58	4.56
CaO	7.60	7.33	8.37	8.85	7.73	9.08	12.20	7.53	8.20	10.00	4.91	6.49	7.88
Na_2O	1.67	3.91	2.82	0.54	3.81	3.02	0.85	3.92	4.05	1.62	5.07	5.21	4.34
K_2O	1.98	0.09	0.97	0.11	0.09	0.09	0.12	0.11	0.07	0.13	0.09	0.11	0.13
P_2O_5	0.09	0.09	0.21	0.06	0.10	0.10	0.12	0.09	0.10	0.08	0.13	0.13	0.19
L.O.I.	0.70	0.47	0.27	1.17	0.30	0.18	0.38	0.34	0.20	0.31	0.20	0.19	0.20
Total	96.30	96.60	96.70	95.30	96.00	96.90	98.10	96.40	97.10	96.40	97.50	97.50	96.40
V (ppm)	190	170	270	160	180	180	180	170	170	160	200	160	230
Cr	610	580	30	1040	590	580	940	540	620	530	30	30	730
Cu	20	340	90	10	30	20	1150	40	10	30	20	20	20
Zn	80	80	150	90	70	70	80	100	90	170	280	180	100
Ni	190	180	50	230	170	160	110	160	180	170	100	90	170
S	460	780	1320	110	180	100	1510	170	120	200	70	210	250
Ba	1210	70	330	60	50	40	30	40	20	30	30	10	50
Sr	240	150	170	170	140	130	600	110	140	180	130	140	170
Zr	110	100	260	80	100	100	130	90	100	100	150	150	130

14 = 196-B-86, 15 = 196-D-86, 16 = 274-B-80, 17 = 357-87, 18 = 272-A-80, 19 = 272-B-80, 20 = 86-A-78, 21 = 87-A-78, 22 = 87-C-78, 23 = 87-D-78, 24 = 357-C-81, 25 = 358-A-81, 26 = 199-A-85

(continued)

Table 1. Continued.

	27	28	29	30	31	32	33	34	35	36	37	38	39
SiO_2	53.60	53.90	56.00	58.60	56.40	58.20	55.10	57.50	58.20	57.00	57.30	56.90	57.90
TiO_2	0.47	0.50	0.59	0.65	0.62	0.62	0.64	0.66	0.64	0.62	0.62	0.58	0.47
Al_2O_3	12.90	13.20	15.80	13.80	14.50	15.00	17.00	15.60	15.00	15.00	14.90	15.10	13.40
$Fe_2O_{3\,tot}$	9.21	9.26	8.83	9.36	10.70	10.00	10.00	9.70	9.03	10.19	9.37	8.37	8.34
MnO	0.16	0.24	0.21	0.18	0.21	0.19	0.16	0.21	0.18	0.19	0.18	0.16	0.13
MgO	8.57	7.96	4.02	4.23	4.73	4.47	3.98	3.74	3.94	4.11	3.76	4.67	6.77
CaO	8.76	7.53	6.26	7.11	6.15	5.06	5.90	5.12	5.45	5.23	6.03	6.41	4.58
Na_2O	2.24	3.66	5.50	3.46	4.11	4.43	4.79	5.38	5.12	5.32	5.08	4.63	2.11
K_2O	0.62	0.09	0.11	0.15	0.13	0.11	0.15	0.11	0.10	0.10	0.13	0.10	3.33
P_2O_5	0.10	0.12	0.14	0.15	0.14	0.12	0.16	0.10	0.15	0.13	0.14	0.12	0.08
L.O.I.	0.54	0.39	0.18	0.19	0.01	0.08	0.01	0.01	0.01	0.01	0.01	0.29	1.00
Total	96.90	96.70	97.50	97.90	97.90	98.30	98.10	98.30	97.90	98.00	97.70	97.20	97.40
V (ppm)	170	160	160	140	160	170	280	150	170	180	180	170	170
Cr	680	600	50	30	30	30	40	30	30	40	30	80	580
Cu	140	10	50	20	40	10	530	60	30	10	90	70	10
Zn	60	240	110	120	140	140	130	140	130	150	150	150	120
Ni	210	200	80	90	90	80	70	90	80	80	80	90	170
S	500	330	200	80	90	70	920	250	170	120	130	320	410
Ba	220	50	30	20	40	30	40	0	40	50	40	40	260
Sr	180	110	120	160	140	120	140	180	160	140	150	160	250
Zr	100	100	130	160	150	140	160	160	160	140	150	140	110

27 = 271-A-80, 28 = 197-A-86, 29 = 360-A-81, 30 = 82-A-78, 31 = 82-B-78, 32 = 82-C-78, 33 = 82-D-78, 34 = 82-E-78, 35 = 82-F-78, 36 = 82-G-78, 37 = 82-H-78, 38 = 85-A-78, 39 = 198-86

	40	41	42	43	44	45	46
SiO_2	57.10	47.80	51.90	51.50	72.00	78.40	70.80
TiO_2	0.46	0.47	1.70	0.50	0.31	0.20	0.34
Al_2O_3	14.30	14.50	13.70	13.30	14.90	12.70	14.70
$Fe_2O_{3\,tot}$	7.95	8.63	12.13	10.03	2.46	0.73	3.81
MnO	0.16	0.21	0.15	0.18	0.02	0.01	0.03
MgO	5.54	6.19	4.14	8.49	1.38	0.32	1.66
CaO	8.26	16.20	8.62	7.59	1.33	0.44	1.11
Na_2O	2.46	0.21	4.26	3.25	3.47	4.48	5.14
K_2O	0.51	0.02	0.44	0.58	2.57	1.58	0.48
P_2O_5	0.10	0.09	0.18	0.09	0.02	0.01	0.10
L.O.I.	0.37	1.55	0.48	0.91	1.11	0.59	1.20
Total	97.20	94.50	97.60	95.80	98.50	99.00	98.40
V (ppm)	190	190	300	180	90	40	90
Cr	540	600	20	610	100	40	130
Cu	20	310	200	10	30	10	350
Zn	50	100	40	80	40	10	60
Ni	120	130	70	180	50	30	60
S	440	550	4110	350	280	100	1550
Ba	370	30	60	260	470	170	90
Sr	430	110	420	130	100	40	70
Zr	120	100	210	100	100	120	150

40 = 196-A-86, 41 = 202-A-86, 42 = 363-A-81, 43 = 274-A-80, 44 = 83-A-78, 45 = 83-B-78, 46 = 84-A-78

Table 2. U-Pb isotopic data. Location of samples are in text and in Figure 1. Hand-picked zircons were analysed in the laboratories of the Geological Survey of Finland. All ages are calculated or recalculated with the decay constants as recommended by Jaffey et al. (1971).

Sample no.	Fraction (g/cm³) Ø = grain size, µm abr = grains abraded	Concentration µg/g ^{238}U	Concentration µg/g ^{206}Pb	$\frac{^{206}Pb}{^{204}Pb}$ measured	Isotopic composition of lead $^{206}Pb = 100$ 204	Isotopic composition of lead $^{206}Pb = 100$ 207	Isotopic composition of lead $^{206}Pb = 100$ 208	Atom ratios and radiometric ages, Ma. $\frac{^{206}Pb}{^{238}U}$	Atom ratios and radiometric ages, Ma. $\frac{^{207}Pb}{^{235}U}$	Atom ratios and radiometric ages, Ma. $\frac{^{207}Pb}{^{206}Pb}$
A185-Kivi-Kiekki, Kuhmo; leucocratic tonalite										
A185A	d>4.6 70<Ø<160	225.6	89.28	2077	.04678	19.133	42.066	.4574 ± 24 2428	11.708 ± 63 2581	.18566 ± 12 2704
B	4.2<d<4.6 70<Ø<160	481.7	162.93	1260	.07883	18.480	7.026	.3910 ± 21 2127	9.440 ± 52 2381	.17512 ± 9 2607
C	d>4.5;Ø<70 abr	304.4	127.45	2646	.03424	19.277	9.865	.4839 ± 32 2544	12.585 ± 86 2649	.18863 ± 22 2730
D	4.0<d<4.2 abr	1039	304.27	1435	.06662	17.207·	4.990	.3385 ± 25 1879	7.642 ± 59 2189	.16374 ± 25 2494
A911-Latvalampi, Kaita-Kiekki, Kuhmo; a granitoid boulder in conglomerate										
A911A	d>4.6	330.5	124.00	2629	.02910	18.130	12.779	.4336 ± 23 2322	10.625 ± 66 2490	.17772 ± 44 2631
B	4.2<d<4.6	443.6	149.04	823.8	.11143	18.587	18.474	.2883 ± 26 2115	9.212 ± 66 2359	.17207 ± 28 2578
C	4.0<d<4.2	680.7	207.70	1003	.09845	17.646	17.843	.3527 ± 21 1947	7.982 ± 49 2228	.16416 ± 12 2499
D	3.8<d<4.0	992.6	235.94	583.3	.16935	17.057	22.998	.2747 ± 15 1564	5.646 ± 34 1923	.14906 ± 32 2335
A913-Pötsölampi, Kuhmo; arkosite (coarse-grained)										
A913A	d>4.2	484.9	114.64	5344	.01346	18.165	14.693	.2733 ± 14 1557	6.782 ± 37 2083	.18001 ± 14 2653
B	4.0<d<4.2 Ø>70	808.9	180.72	4805	.01897	17.539	14.423	.2582 ± 13 1480	6.161 ± 33 1998	.17305 ± 18 2587
C	3.8<d<4.0	1155	206.79	1551	.06061	17.028	16.089	.2070 ± 11 1212	4.644 ± 25 1757	.16274 ± 12 2484
D	4.0<d<4.2 violet; abr	653.7	212.24	4177	.02262	17.825	14.864	.3753 ± 19 2054	9.079 ± 48 2346	.17549 ± 10 2610
E	4.0<d<4.2 yellowish Ø>130; abr	547.1	170.10	3108	.03024	18.383	16.972	.3593 ± 23 1979	8.925 ± 59 2330	.18016 ± 15 2654
F	4.0<d<4.2 euhedral; dark Ø>130; abr	725.2	236.40	3843	.02374	17.743	13.901	.3767 ± 22 2060	9.065 ± 54 2344	.17453 ± 23 2601

Table 2. Continued.

Sample no.	Fraction (g/cm³) Ø = grain size, μm abr = grains abraded	Concentration μg/g ^{238}U	^{206}Pb	$\dfrac{^{206}Pb}{^{204}Pb}$ measured	Isotopic composition of lead $^{206}Pb = 100$ 204	207	208	Atom ratios and radiometric ages, Ma. $\dfrac{^{206}Pb}{^{238}U}$	$\dfrac{^{207}Pb}{^{235}U}$	$\dfrac{^{207}Pb}{^{206}Pb}$
	A912-Pötsölampi, Kuhmo; arkosite (fine-grained)									
912A	4.0 < d < 4.2	878.1	177.25	2145	.04380	17.838	18.304	.2333 ± 12 1351	5.564 ± 30 1910	.17296 ± 12 2586
B	3.8 < d < 4.0 Ø > 70	1268	198.35	1842	.05162	16.973	18.142	.18082 ± 94 1071	4.071 ± 22 1648	.16328 ± 10 2490
C	d > 4.2	502.2	115.60	2119	.03983	18.621	18.563	.2660 ± 14 1520	6.651 ± 37 2066	.18133 ± 22 2665
D	4.0 < d < 4.2 abr	559.4	190.63	7524	.01131	17.913	15.309	.3939 ± 64 2140	9.65 ± 16 2402	.17774 ± 30 2632
	A186-Saari-Kiekki, Kuhmo; granitoid boulder in the volcanic conglomerate									
A186A	3.8 < d < 4.0 abr	1384	361.75	189.5	.52614	20.048	35.144	.3021 ± 17 1701	5.516 ± 39 1903	.13245 ± 48 2130
B	d > 4.0; abr	806.5	249.48	351.7	.27704	18.666	21.550	.3575 ± 33 1970	7.471 ± 73 2169	.15157 ± 41 2363
C	3.8 < d < 4.0 abr	1751	463.30	267.5	.37187	18.287	27.113	.3059 ± 22 1720	5.689 ± 43 1929	.13492 ± 23 2163
D	3.6 < d < 3.8 abr	1089	217.89	251.4	.39073	17.486	30.870	.2312 ± 19 1340	3.949 ± 36 1623	.12387 ± 40 2012
E	3.6 < d < 4.0 abr	1386	313.53	239.9	.40977	18.400	28.735	.2614 ± 18 1496	4.718 ± 35 1770	.13093 ± 30 2110
F	titanite 3.4 < d < 3.5 abr	58.11	21.08	94.2	1.0598	25.622	68.603	.4193 ± 24 2257	6.57 ± 12 2055	.1136 ± 17 1858
G	titanite 3.5 < d < 3.6 abr	47.17	17.56	93.0	1.0730	25.859	66.757	.4302 ± 26 2306	6.71 ± 11 2073	.1131 ± 17 1850
H	titanite 3.4 < d < 3.5 abr	45.23	13.59	131.9	.75374	21.228	48.724	.3472 ± 19 1921	5.252 ± 55 1861	.10970 ± 85 1794
	A261-Rasiaho, Saari-Kiekki, Kuhmo; metadiabase									
A261A	4.3 < d < 4.6 Ø < 100	289.6	60.43	443.6	.22203	15.010	59.151	.2412 ± 17 1392	4.000 ± 48 1634	.1203 ± 10 1961
B	4.3 < d < 4.6 Ø > 100; abr	274.9	59.61	429.1	.23007	14.939	76.875	.2506 ± 15 1441	4.093 ± 30 1652	.11847 ± 44 1933
C	4.0 < d < 4.2 abr	605.7	137.61	793.2	.12455	13.612	63.788	.2626 ± 17 1503	4.325 ± 31 1698	.11947 ± 29 1948

Table 2. Continued.

Sample no.	Fraction (g/cm³) Ø = grain size, μm abr = grains abraded	Concentration μg/g		206Pb/204Pb measured	Isotopic composition of lead 206Pb = 100			Atom ratios and radiometric ages, Ma.		
		238U	206Pb		204	207	208	206Pb/238U	207Pb/235U	207Pb/206Pb
D	4.3 < d < 4.6 abr; crushed	286.4	63.07	432.7	.22936	15.007	73.104	.2545 ± 24 1461	4.185 ± 47 1671	.11927 ± 59 1945
E	4.3 < d < 4.6 yellowgreen abr	270.0	59.68	1486	.05451	12.269	28.499	.2555 ± 16 1466	4.063 ± 31 1646	.11534 ± 37 1885
F	4.3 < d < 4.6 Ø > 160; abr	269.4	57.68	438.1	.22192	14.578	39.825	.2474 ± 21 1425	3:953 ± 36 1624	.11586 ± 30 1893
G	4.2 < d < 4.3 abr	361.3	78.64	675.8	.14551	13.906	73.362	.2516 ± 15 1446	4.149 ± 26 1664	.11961 ± 18 1950
H	4.0 < d < 4.3 light coloured abr	447.0	97.22	760.0	.12353	13.733	42.568	.2514 ± 53 1445	4.189 ± 89 1671	.12084 ± 29 1968
I	3.8 < d < 4.0 translucent abr	1412	377.49	2178	.04451	13.916	62.579	.3090 ± 20 1735	5.679 ± 37 1928	.13330 ± 18 2142
J	titanite 3.5 < d < 3.6	22.10	6.99	108.6	.91347	25.743	135.99	.3657 ± 19 2009	6.951 ± 49 2105	.13784 ± 55 2200
K	titanite 3.5 < d < 3.6 abr	20.07	6.85	150.7	.65514	22.325	137.18	.3947 ± 31 2144	7.479 ± 69 2170	.13744 ± 52 2195
L	3.8 < d < 4.0 translucent Ø > 70; abr	1298	352.95	2122	.04473	13.711	73.093	.3142 ± 18 1761	5.683 ± 33 1928	.13121 ± 10 2114

References

Arndt, N.T. and Jenner, G.A., 1986. Crustally contaminated Komatiites and Basalts from Kambalda, Western Australia. Chemical Geol.,56, 229—255.

Carter, R.M. & Norris, R.J., 1976. Cainozoic history of southern New Zealand: an accord between geological observations and plate-tectonic predictions. Earth Planet. Sci. Letts, 31, 85—94.

Condie, K.C., 1985. Secular Variation in the Composition of Basalts: an Index to Mantle Evolution. J. of Petrol., vol.26, Part 3,545—546.

Eskola, P.E., 1919. Huvuddragen av Onega-Karelens geologi. Teknikern, 1919, 37—39.

—, 1941. Erkki Mikkola und der heutige stand der präkambrischen Geologie in Finland. Geologishe Rundschau Bd. 32. Heft 4/5.

—, 1963. The Precambrian of Finland. In: K. Rankama (Ed) The Precambrian, vol. 1, John Wiley & Sons Inc. New York-London-Sydney.

Fowler, A.D., Jensen, L.S. and Peloquin, S.A., 1987. Variolites in Archaean basalts: products of spherulitic crystallization. Canadian Mineralogist. Vol. 25, 275—289.

Gill, J.B., 1981. Orogenic andesites and plate tectonics. Springer-Verlag, New York. 390 p.

Harding, T.P., 1985. Seismic Characteristics and Identification of Negative Flower Structures, Positive Flower Structures, and Positive Structural Inversion. Am. Ass. Petrol. Geol. Bull., vol. 69, No 4. 582—600.

Hempton, M.R., Dunne, L.A. and Dewey, J.F., 1983. Sedimentation in an active strike-slip basin, southeastern Turkey. J. Geology, 91, 401—412.

Huppert, H.E., Sparks, R.S.J., Turner, J.S. and Arndt, N.T., 1984. Emplacement and cooling of Komatiite lava. Na-

186   *Erkki J. Luukkonen*

ture (London), 309, 19—22.
—, & *Sparks, R.S.J.,* 1985. Cooling and contamination of mafic and ultramafic lavas during ascent through continental crust. Earth Planet. Sci. Lett.,74, 371—386.
—, 1988. The Generation of Granitic Magmas by Intrusion of Basalt into Continental Crust. J. of Petrol., vol.29, Part 3, 599—624.
Hyppönen, V., 1983. Kallioperäkarttojen selitykset, 4411 Ontojoki, 4412 Hiisijärvi ja 4413 Kuhmo. English summary: Pre-Qarternary rocks of the Ontojoki, Hiisijärvi and Kuhmo map sheet areas. Geological map of Finland 1: 100 000. Espoo: Geological Survey of Finland. 60p.
Irvine, T.N. and Baragar, W.R.A., 1971. A guide to the chemical classification of the common volcanic rocks. Can. J. Earth Sci., 8. 523—548.
Jaffey, A.H., Flynn, K.F., Glendenin, L.E., Bentley, W.C. & Essling, A., 1971. Precision measurement of half-lives and specific activities of ^{235}U and ^{238}U. Phys. Rev C4, 1889—1906.
Jensen, L.S., 1976. A new cation plot for classifying subalkalic volcanic rocks. Ont. Dep. Min. Misc. Pap. 66, 22 p.
Kratz, K.O., 1976. Age range of the Jatulian Complex of Karelia. Dokl. Acad. Nauk. SSSR, Earth Sci, Sect, 231, (5), 1191—1194.
— & *Mitrofanov, F.,* 1980. Main type reference sequences of the early Precambrian in the U.S.S.R. Earth Sci Review. 16. 295—301.
Kilpelä, M., 1990. Karttalehtien 4421, 4423 + 4441 alueen metadiabaaseista. Pro gradu -tutkielma. Geologian ja mineralogian laitos, Turun yliopisto. in preparation.
Kulikov, V.S. & Golubev, A.I., 1984. The Sumian-Sariolan. In: V.A.Sokolov (ed.) GUIDE-BOOK Geological field trips in Karelia. Institute of Geology Academy of Sciences of the USSR Karelian Branch. Petrozavodsk 1984. 15—18.
Laajoki, K., 1973. On the geology of the South Puolanka area, Finland. Geol. Surv. Finland, Bull. 263. 54 p.
—, 1980. Outlines of the Precambrian geology of the North Puolanka area, Finland. Res Terrae, Ser. A. 1. 11p.
Luukkonen, E.J., 1985. Structural and U-Pb isotopic study of late Archaean migmatitic gneisses of the Presvecokarelides, Lylyvaara, eastern Finland. Trans. R. Soc. Edinburgh Earth Sci. 76, 401—410.
—, 1988a. The structure and stratigraphy of the northern part of late Archaean Kuhmo greenstone belt, eastern Finland. In E. Marttila (ed.) Archaean geology of the Fennoscandian Shield, 71—96. Geol. Surv. Finland, Spec. Paper 4.
—, 1988b. Kallioperäkarttojen selitykset, 4421 Moisiovaara ja Ala-Vuokki. English summary: Pre-Quarternary rocks of the Moisiovaara and Ala-Vuokki map sheet areas. Geological map of Finland 1: 100 000. Espoo, Geological Survey of Finland.
— & *Lukkarinen, H.,* 1986. Explanation to the stratigraphic map of Middle Finland. Geol. Surv. Finland Rep. Inv.

74, 47p.
Marmo, J.S., 1986. Sariolan stratigraphy and sedimentation in the Koli-Kaltimo area, North Karelia, eastern Finland. In V. Sokolov (ed.) Proceedings of Symposium on the lower Proterozoic formations on the eastern part of the Baltic Shield, Petrozavodsk, 1985.
Marmo, J.S. & Ojakangas, R.W., 1983. Varhaisproterosooinen Urkkavaara-muodostuma Kontiolahdella; glasigeeninen metasedimenttisarja sariolaryhmän yläosassa. Summary: Early Proterozoic Urkkavaara Formation in Kontiolahti, North Karelia — A glacigenic metasedimentary sequence in the upper Sariolan group. Geologi 35, 27—29.
—, 1984. Lower Proterozoic glaciogenic deposits, eastern Finland. Geol.Soc.Am.Bull.95, 1055—1062.
—; *Kohonen, J., Sarapää, O. & Äikäs, O.,* 1988. Sedimentology and stratigraphy of the lower Proterozoic Sariola and Jatuli Groups in the Koli-Kaltimo area, eastern Finland. In: K.Laajoki and J.Paakkola (eds) Sedimentology of the Precambrian formations in eastern and northern Finland. Geol. Surv. Finl. Spec. Paper 5. 11—28.
Meriläinen, K., 1980. On the stratigraphy of the Karelian formations. In A. Silvennoinen (ed.) Jatulian geology in the eastern part of the Baltic Shield. Proceedings of a Finnish-Soviet Symposium, Finland, 1979, 9—12. See also Stratigraphy of the Precambrian in Finland. Geol.Fören. Stockholm Förh. 102(2), 177—180.
Nardin, T.R. & Henyey, T.L., 1978. Pliocene-Pleistocene diastrophism of Santa Monica and San Pedro shelves, California continental Borderland. Bull.Am.Ass.Petrol.Geol. 62, 247—272.
Nesbitt, H.W. & Young, G.M., 1982. Early Proterozoic climates and plate motions inferred from major element chemistry of lutites. Nature, vol.299, No. 5885, 715—717.
Norris, RJ., Carter, R.M. & Turnbull, I.M., 1978. Cainozoic sedimentation in basins adjacent to a major continental transform boundary in southern New Zealand. J.geol. Soc.Lond.135, 191—205.
Ojakangas, R.W., 1965. Petrography and sedimentation of the Precambrian Jatulian quartzites of Finland. Bull.Comm.geól. Finlande 214, 74p.
Park, A.F., Bowes, D.R., Halden, N.M. & Koistinen, T.J., 1985. Tectonic evolution at an early Proterozoic continental margin: the Svecokarelides of eastern Finland. J. Geodynamics 1, 359—386.
Paerce, J.A., 1983. Role of the Sub-continental Lithosphere in Magma Genesis at Active Continental Margins. In: C.J.Hawkesworth and M.J.Norry (Eds.), Continental Basalts and Mantle Xenoliths. Shiva Press, Nantwich, 230—249.
Pekkarinen, L.J., 1979. The Karelian formations and their depositional basement in the Kiihtelysvaara — Värtsilä area, East Finland. Geol.Surv.Finland,Bull. 301, 141p.
Pettijohn, F.J., 1975. Sedimentary Rocks. Harber & Row, Publishers, New York-Evanston-San Francisco-London.

628 p.

Ramsay, J.G. and Huber, M.I., 1987. The Techniques of Modern Structural Geology, vol. 2: Folds and Fractures. Academic Press; Harcourt Brace Jovanovich, Publishers, 699 p.

Reading, H,G., 1980. Characteristics and recognition of strike-slip fault systems. Spec. Publ. int. Ass. Sediment.4, 7—26.

Sokolov, V.A. & Stenar, N.M., 1980. Prinzipy ia i korrelatzyi dokekambrija jugo-vostoshnoi chasti Baltijkogo skita. Prinzipy i kriteri dokembrija v mobilńykh zonakh, Leningrad (with English and French abstracts).

Strand, K., 1985. Alaproterosooisen Kurkikylän ryhmän ja sen päällä olevien karjalaisten muodostumien litostratigrafia, paleosedimentologia ja rakenne. Res Terrae Ser. B 7. 140 p.

—, 1988. Alluvial sedimentation and tectonic setting of the early Proterozoic Kurkikylä and Kainuu Groups in northern Finland. In: Laajoki,K. and Paakkola,J. (eds) Sedimentalogy of the Precambrian formations in eastern and northern Finland. Geol. Spec. Paper 5. 75—90.

Sylvester, A.G., 1988. Strike-slip faults. Geol. Soc. Am. Bull. v.100. 1666—703.

Taylor, S.R. & McLennan, S.M., 1981. The composition and evolution of the continental crust: rare earth evidence from sedimentary rocks. Philos.Trans. R. Soc. London, ser. A, 301. 381—399.

Thompson, R.N., Morrison, M.A., Dickin, A.P. & Hendry, G.L., 1983. Continental Flood Basalts Arachnids Rule OK ? In: C.J. Hawkesworth and M.J.Norry (Eds.), Continental Basalts and Mantle Xenoliths. Shiva Press, Nantwich, 158—185.

Viljoen, R.P. & Viljoen, M.J., 1982. Komatiites: a historical review. In N.T. Arndt and E.G.Nisbett (eds), Komatiites, George Allen and Unwin, London, 5—18.

Väyrynen, H., 1933. Über die Stratigrafie der karelischen Formationen. Bull. Comm. geól. Finlande 101, 54—78.

—, 1954. Suomen kallioperä, sen synty ja geologinen kehitys. Otava, Helsinki. 260p.

Wilkman, W.W., 1921. Vuorilajikartan selitys D 4, Nurmes. 126 p.

Zhuravlev, V.A., Ivanov, N.M., Negrutza, V.Z., Negrutza, T.F. & Pushkin, G.J., 1979. Prejatulian formations of the link zone between Karelides and Belomorides. In A. Silvennoinen (ed.) Jatulian geology in the eastern part of the Baltic Shield. Proceedings of a Finnish-Soviet Symposium, Finland, 1979, 239—251.